PB81-112872

Physical Chemistry of Virus Adsorption and Degradation on Inorganic Surfaces Its Relation to Wastewater Treatment

Stanford Univ. CA

Prepared for

Municipal Environmental Research Lab
Cincinnati, OH

Aug 80

U.S. Department of Commerce
National Technical Information Service
NTIS.

United States
Environmental Protection
Agency

Municipal Environmental Research
Laboratory
Cincinnati OH 45268

EPA-600/2-80-134
August 1980

Research and Development

PB81-112872

EPA

Physical Chemistry of Virus Adsorption and Degradation on Inorganic Surfaces

Its Relation to Wastewater Treatment

REPRODUCED BY
NATIONAL TECHNICAL
INFORMATION SERVICE
U. S. DEPARTMENT OF COMMERCE
SPRINGFIELD, VA. 22161

RESEARCH REPORTING SERIES

Research reports of the Office of Research and Development, U.S. Environmental Protection Agency, have been grouped into nine series. These nine broad categories were established to facilitate further development and application of environmental technology. Elimination of traditional grouping was consciously planned to foster technology transfer and a maximum interface in related fields. The nine series are:

1. Environmental Health Effects Research
2. Environmental Protection Technology
3. Ecological Research
4. Environmental Monitoring
5. Socioeconomic Environmental Studies
6. Scientific and Technical Assessment Reports (STAR)
7. Interagency Energy-Environment Research and Development
8. "Special" Reports
9. Miscellaneous Reports

This report has been assigned to the ENVIRONMENTAL PROTECTION TECHNOLOGY series. This series describes research performed to develop and demonstrate instrumentation, equipment, and methodology to repair or prevent environmental degradation from point and non-point sources of pollution. This work provides the new or improved technology required for the control and treatment of pollution sources to meet environmental quality standards.

This document is available to the public through the National Technical Information Service, Springfield, Virginia 22161.

TECHNICAL REPORT DATA
(Please read Instructions on the reverse before completing)

1. REPORT NO EPA-600/2-80-134	2.
3. RECIPIENT'S ACCESSION NO. PB81 112872	
4. TITLE AND SUBTITLE PHYSICAL CHEMISTRY OF VIRUS ADSORPTION AND DEGRADATION ON INORGANIC SURFACES Its Relation to Wastewater Treatment	5. REPORT DATE August 1980 (Issuing Date) 6. PERFORMING ORGANIZATION CODE
7. AUTHOR(S) James P. Murray	8. PERFORMING ORGANIZATION REPORT NO.
9. PERFORMING ORGANIZATION NAME AND ADDRESS Department of Applied Earth Sciences Stanford University Stanford, California 94305	10. PROGRAM ELEMENT NO. P.E.35B1C A/14 11. CONTRACT/GRANT NO. R-805016
12. SPONSORING AGENCY NAME AND ADDRESS Municipal Environmental Research Laboratory--Cin.,OH Office of Research and Development U.S. Environmental Protection Agency Cincinnati, Ohio 45268	13. TYPE OF REPORT AND PERIOD COVERED Final Sept. 1976-March 1978 14. SPONSORING AGENCY CODE EPA/600/14

15. SUPPLEMENTARY NOTES

Project Officer: Albert D. Venosa (513) 684-7668

16. ABSTRACT

The DLVO-Lifshitz theory of colloid stability is applied to adsorption of poliovirus on oxide surfaces common in soil and aquatic environments. Excellent agreement was found between colloid stability theory and adsorption free energies calculated from mass-action principles. Colloid stability theory now provides an organized frame of reference with which to understand virus adsorption in the environment. On some surfaces, notably β-MnO_2, CuO, and Al metal, kinetic analysis of data from multiple extractions and sedimentation analysis reveals that virus was actually degraded by adsorption. A column experiment also indicated that Al metal also effectively degraded virus in the presence of secondary wastewater effluent. Potential applications to wastewater treatment are suggested.

This report was submitted in fulfillment of Grant No. R-805016 by Stanford University under the sponsorship of the U.S. Environmental Protection Agency. This report covers the period September 1, 1976 to March 1, 1978.

17. KEY WORDS AND DOCUMENT ANALYSIS

a. DESCRIPTORS	b. IDENTIFIERS/OPEN ENDED TERMS	c. COSATI Field/Group
Physical chemistry, Adsorption, Adsorbents, Desorption, Viruses, Disinfection, Waste treatment, Aluminum inorganic compounds, Copper inorganic compounds, iron inorganic compounds, silicon inorganic compounds	Colloid stability theory, Van der Waals forces, Double layer interaction, Virus inactivation, Virus adsorption	07D 0GM 13B

18. DISTRIBUTION STATEMENT Release to Public	19. SECURITY CLASS *(This Report)* Unclassified 20. SECURITY CLASS *(This page)* Unclassified	21. NO. OF PAGES 22. PRICE

EPA Form 2220-1 (9-73)

☆ U.S. GOVERNMENT PRINTING OFFICE: 1980--657-165/0125

EPA-600/2-80-80-134
August 1980 30

PHYSICAL CHEMISTRY OF VIRUS ADSORPTION AND DEGRADATION ON INORGANIC SURFACES

Its Relation to Wastewater Treatment

by

James P. Murray
Stanford University
Stanford, California 94305

Grant No. R-805016

Project Officer

Albert D. Venosa
Wastewater Research Division
Municipal Environmental Research Laboratory
Cincinnati, Ohio 45268

MUNICIPAL ENVIRONMENTAL RESEARCH LABORATORY
OFFICE OF RESEARCH AND DEVELOPMENT
U.S. ENVIRONMENTAL PROTECTION AGENCY
CINCINNATI, OHIO 45268

DISCLAIMER

This report has been reviewed by the Municipal Environmental Research Laboratory, U.S. Environmental Protection Agency, and approved for publication. Approval does not signify that the contents necessarily reflect the views and policies of the Environmental Protection Agency, nor does mention of trade names or commercial products constitute endorsement or recommendation for use.

FOREWORD

The U.S. Environmental Protection Agency was created because of increasing public and government concern about the dangers of pollution to the health and welfare of the American people. Noxious air, foul water, and spoiled land are tragic testimonies to the deterioration of our natural environment. The complexity of that environment and the interplay of its components require a concentrated and integrated attack on the problem.

Research and development is that necessary first step in problem solution; it involves defining the problem, measuring its impact, and searching for solutions. The Municipal Environmental Research Laboratory develops new and improved technology and systems to prevent, treat, and manage wastewater and solid and hazardous waste pollutant discharges from municipal and community sources, to preserve and treat public drinking water supplies, and to minimize the adverse economic, social, health, and aesthetic effects of pollution. This publication is one of the products of that research and provides a most vital communications link between the researcher and the user community.

This report presents a detailed fundamental investigation of the mechanisms that control adsorption of viruses to mineral surfaces in the environment. The findings have important implications regarding which natural soil and aquatic systems are conducive to viral dissemination and those that are not. In addition, application of the optimum adsorbent for wastewater purification and water recycling was investigated in detail. Promising results were obtained that could eventually lead to the development of a new nontoxicogenic water reclamation process.

Francis T. Mayo
Director
Municipal Environmental Research
Laboratory

ABSTRACT

The DLVO-Lifshitz theory of colloid stability was applied to adsorption of poliovirus on oxide surfaces common in soil and aquatic environments. Excellent agreement was found between colloid stability theory and adsorption free energies calculated from mass-action principles. Colloid stability theory now provides an organized frame of reference with which to understand virus adsorption in the environment. On some surfaces, notably β-MnO_2, CuO, and Al metal, kinetic analysis of data from multiple extractions and sedimentation analysis reveals that virus was actually degraded by adsorption. A column experiment also indicated that Al metal also effectively degraded virus in the presence of secondary wastewater effluent. Potential applications to wastewater treatment are suggested.

This report was submitted in fulfillment of Grant No. R-805016 by Stanford University under the sponsorship of the U.S. Environmental Protection Agency. This report covers the period September 1, 1976 to March 1, 1978.

CONTENTS

Foreword iii
Abstract iv
Figures. vi
Tables vii
Abbreviations and Symbols. ix
Acknowledgements xii

1. Introduction 1
   Project Objectives 1
   Importance of Problem and Review of Previous Work. . . . 1
2. Conclusions. 4
3. Recommendations. 5
4. Materials and Methods. 6
   Virus and Assay. 6
   Statistics of Assay Data 7
   Buffers. 8
   Adsorbents 8
   Chemicals, Isotopes, and Analytical Methodology. 9
5. Mechanism of Poliovirus Adsorption 11
   Thermodynamic Approach 11
   Determination of ΔG_{ads} 11
   Application of DLVO-Lifshitz Theory. 21
   Electrostatic Components of ΔG_{ads}. 22
   Electrodynamic Components of ΔG_{ads}. 28
   Other Possible Components. 32
   Predictions from DLVO-Lifshitz Theory. 33
6. Degradation of Poliovirus by Adsorption. 36
   Kinetic Approach 36
   Degradation Experiments. 38
   Results. 40
   Degradation by Aluminum Metal. 44
   Discussion 48
7. Application of Aluminum Metal to Wastewater Decontamination. 53
   Introduction 53
   Bench-Scale Process Experiment 53
   Results. 56
   Discussion 58

References 60

FIGURES

Number		Page
1	Adsorption and degradation apparatus	14
2	Adsorption-desorption isotherms of poliovirus on oxides at 0.02 ionic strength and pH 7	18
3	Adsorption-desorption isotherms of poliovirus on oxides at 0.305 ionic strength and pH 7	19
4	Adsorption-desorption isotherms of poliovirus on Al_2O_3 and aluminum metal at 0.02 ionic strength and pH 7	20
5	Diagrammatic representation of double layers about virus and solid.	23
6	Variation of poliovirus adsorption with pH and α-SiO_2 at 0.02 ionic strength as predicted by DLVO theory	34
7	Kinetic plot for α-Fe_2O_3 Sample C.	43
8	Kinetic plot for β-MnO_2 Sample C	45
9	Kinetic plot for CuO Sample C	46
10	Kinetic plot for α-Al_2O_3 Sample C	49
11	Kinetic plot for Al Metal Sample C	50
12	Sedimentation profiles of virus degraded by Al metal	51
13	Schematic diagram of bench-scale process experiment.	54
14	Photograph of bench-scale process experiment	55
15	Results from process experiment.	57

TABLES

Number		Page
1	Surface Areas of Adsorbents	16
2	Free Energies of Poliovirus Adsorption on Oxide Surfaces as Determined by Mass-Action Equilibria.	21
3	Normalized Concentration of Poliovirus Infectivity in Equilibrium with Various Solids	22
4	Zeta Potentials of Oxides and Virus in pH 7 $NaHCO_3$-NaCl Solutions	26
5	Comparison of Theoretical Isoelectric Points with Values Reported for Other Enteroviruses	27
6	Double Layer Interaction Potentials between Virus and Solid Phases According to the LSA Expression	27
7	Comparison of Differences in ΔG_{ads} and U_{dl} at 0.02 I and 0.305 I	28
8	Individual Self-Interaction Hamaker Coefficients Taken from Visser (65) and Calculated Mixed Coefficients	31
9	Comparison of Lifshitz-Van der Waals Potentials to Residual Free Energy Components after Correcting for Double-Layer Repulsion	31
10	Comparison of Virus Initially Adsorbed (Ads_i) with Virus Recovered (Ads_r) for α-SiO_2	41
11	Comparison of Virus Initially Adsorbed (Ads_i) on α-Fe_2O_3 with Virus Recovered by Kinetic Analysis of Data from Four Extractions (Ads_o)	42
12	Comparison of Virus Initially Adsorbed (Ads_i) on β-MnO_2 with Virus Recovered by Kinetic Analysis of Data from Four Extractions (Ads_o).	44
13	Comparison of Virus Initially Adsorbed (Ads_i) on CuO with Virus Recovered by Kinetic Analysis of Data from Four Extractions (Ads_o).	47

Number		Page
14	Comparison of Virus Initially Adsorbed (Ads_i) on α-Al_2O_3 with Virus Recovered by Kinetic Analysis of Data from Four Extractions (Ads_o)	48
15	Comparison of Virus Initially Adsorbed (Ads_i) on Al Metal with Virus Recovered by Kinetic Analysis of Data from Four Extractions (Ads_o)	52
16	Composition of Composite Secondary Effluent (Unchlorinated) Obtained from Palo Alto Sewage Treatment Plant	56

LIST OF ABBREVIATIONS AND SYMBOLS

ABBREVIATIONS

ACS	–	American Chemical Society
BET	–	Brunauer, Emmett, and Teller isotherm for surface area measurement
CPM	–	counts per minute
COD	–	chemical oxygen demand
DLVO	–	Derjaguin, Landau, Verwey and Overbeek theory of colloid stability
ddd H_2O	–	double distilled deionized water
g	–	gram, gravitational unit (acceleration)
Hz	–	Hertz, cycles per second
I	–	ionic strength
kJ/mol	–	kilojoules per mole
LSA	–	linear superposition constant charge assumption
M	–	molar
MEM	–	minimal essential medium
ND	–	not determined
PFU	–	plaque-forming unit
SD	–	standard deviation
s	–	second
THM	–	trihalomethane
U	–	international unit, e.g. for concentration of penicillin

SYMBOLS

$A_{11,22,33}$	–	individual self-interaction Hamaker coefficients for Van der Waals potential calculation
$A_{132,131}$	–	complex Hamaker coefficients
Ads_i	–	virus initially adsorbed
$Ads_{n,n-1}$	–	virus adsorbed after extraction sequence n, n-1
Ads_o	–	virus recoverable with an infinite number of extractions
Ads_r	–	virus recovered after elution from SiO_2
$Ads_{1,2}$	–	virus adsorbed after adsorption (1), desorption (2) in mechanism experiments
a_v	–	virion radius, poliovirus = 27 nm
b	–	background counts in scintillation counting
b_i	–	fitting coefficient ~0.32 x 10-16/s, for Bargeman and Van Voorst Vader theory
C_e	–	virus concentration after elution from SiO_2
C_{eq}	–	equilibrium concentration of virus in liquid phase
C_{H_2O}	–	water concentration in solution, mol/kg
C_{in}	–	concentration entering column
C_n	–	virus concentration in elution medium after extraction sequence n

C'_n – C_n minus virus left over from previous extraction
C_{out} – concentration leaving column
C_u – virus concentration not adsorbed after adsorption step for degradation studies with SiO_2
c – velocity of electromagnetic radiation in vacuum
χ – integration variable for Lifshitz function
d_{ed} – characteristic equilibrium separation for electrodynamic forces
d_{es} – characteristic equilibrium separation distance for electrostatic interaction
ΔG_{ads} – free energy of adsorption-Gibbs function
$\Delta G_{cov\text{-}ion}$ – covalent-ionic bond contribution to ΔG_{ads}
ΔG_{dl} – double layer contribution to ΔG_{ads}
ΔG_{res} – residual energy after subtracting U_{dl} from ΔG_{ads}
ΔG_{VdW} – Van der Waals contribution to ΔG_{ads}
ΔS_o – entropy considerations in ΔG_{ads} not accounted for in other terms
Δt – time intervals between extraction sequences
e – electronic charge
ε_o – zero frequency dielectric constant relative to vacuum
ε_v – dielectric permittivity of free space
$\varepsilon_{1,2,3}$ – complex frequency dependent dielectric susceptibility function of materials 1,2,3
ε' – real coefficient of $\varepsilon_{1,2,3}$
ε'' – imaginary coefficient of $\varepsilon_{1,2,3}$
F – Faraday's constant
F_{ads} – fraction of virus adsorbed
F_{132} – electrodynamic induction force (Van der Waals) between materials 1 and 2, immersed in medium 3
$\gamma_{1,2}$ – $\tanh(y_{1,2}/4)$
i – imaginary modulus $(-1)^{1/2}$
k – rate constant
k_B – Boltzmann's constant
κ – Debye inverse length = $(2e^2nz^2/\varepsilon_o\varepsilon_v k_B T)^{1/2}$
m – number of pipetting operations
N – number of counts or plaques in statistical evaluation
N_a – Avogadro's number
n – extraction sequence number in degradation studies
$n_-; n_+$ – anion or cation number (per m^3) in double layer formulations
ω – complex frequency $\omega_R + i\varepsilon$
ω_R – real part of ω
ω_{132} – value of complex Lifshitz frequency integral
PI – packing index virions per m^2
$PFU/ml_{1,2}$ – 1 refers to titer in adsorption supernatant, 2 to desorption supernantant
PPR – virus particle to PFU ratio
pH_{PZC} – pH where particle (virus) has no net charge
ppb – parts per billion
ψ_o – surface potential
$\psi_{1,2}$ – Stern potential of particle 1,2
R – gas constant
S_a – specific surface area of adsorbent
σ – theoretical standard deviation
T – temperature

Tot	–	total virus in system
t	–	time
θ	–	fraction of surface covered
U_{dl}	–	double layer interaction potential energy
U_{VdW}	–	Van der Waals interaction potential energy
V_a	–	volume during adsorption step
V_d	–	volume during desorption step
V_e	–	volume during elution with SiO_2
V_n	–	volume during extraction sequence n
V_r	–	residual solution volume left over from adsorption step or previous extraction
w_a	–	weight of adsorbent
w_r	–	weight of adsorbent remaining after initial sampling in degradation studies on SiO_2
x	–	water molecules desorbed per virion adsorbed in mechanism studies
x	–	sequence number for final extraction
$y_{1,2}$	–	$ze\psi_{1,2}/k_BT$
z	–	charge of anion or cation
$\zeta_{1,2}$	–	zeta potential of substances 1, 2

ACKNOWLEDGEMENTS

The first section of this report, which defines the mechanisms by which poliovirus adsorbs to various materials, was the subject of the Ph.D. dissertation of the author. In this regard, financial assistance by Mr. John L. Murray, Dr. John R. Murray, Dr. H.H. Huang, and Sigma-Xi is acknowledged. The U.S. Environmental Protection Agency supported the concluding phase of the dissertation, degradation studies, and bench scale process experiments.

The advice and laboratory space provided by Drs. G.A. Parks, C.E. Schwerdt, and P.L. McCarty are much appreciated. Dr. R.O. James, currently at the C.S.I.R.O. Textile Physics Div., Ryde, N.S.W., Australia, assisted with fundamental concepts of the DLVO-Lifshitz theory. Dr. B.D. Korant and K. Lonberg-Holm are thanked for permission to cite unpublished data. S. Enriquez, S. Laband, M. Sanchez, E. Slack, and E. Terehoff are thanked for technical assistance. Especial thanks belongs to the Division of Applied Sciences, Ms. Ellen Campbell and Ms. Dot Franzosa of Harvard University for assistance with final report preparation.

SECTION 1

INTRODUCTION

PROJECT OBJECTIVES

The objectives of this investigation were to determine how potentially pathogenic enteric viruses adsorb to mineral surfaces in the environment, to investigate and quantify actual degradation of virus by adsorption to various surfaces, and to apply information obtained from the first two studies towards development of a virus removal process applicable to water purification and wastewater reclamation.

IMPORTANCE OF PROBLEM AND REVIEW OF PREVIOUS WORK

A recent survey conducted by Dr. Martin Goldfield (1) of the New Jersey Department of Health indicates that viral disease, particularly viral gastroenteritis and infectious hepatitis, continues to be transmitted through contaminated water even in the United States. Virus transmission problems are an active environmental concern. The massive epidemics of waterborne hepatitis in Delhi, India, in 1955, involving 35,000 cases (2) and of waterborne Salmonella typhimurium in Riverside, Calif., in 1965, involving 16,000 cases (3) point to potential hazards associated with waterborne disease.

Problems associated with the problem of controlling viruses in water have been reviewed by Dr. Gerald Berg of the U.S. Environmental Protection Agency (4).

Enteric viruses have been isolated from raw and treated domestic effluents and in relatively uncontaminated water (5). Even low levels may be considered significant because exceptionally low titers of virus, e.g. 2 plaque forming units (PFU) with poliovirus type 1, strain SM (6), have been shown to infect human volunteers. The question of what levels of removal are required to prevent transmission of disease by drinking water has yet to be defined.

In soil and aquatic environments, adsorption of enteroviruses to various mineral surfaces appears to be a major control on virus dispersal in the environment. Pioneering work on this topic was done at Stanford by Drewry and Ryan (7,8). They showed that coliphages T1, T2, and T5 were rapidly taken up by soil and sand columns, and that soil columns, especially those made with soils containing abundant clay minerals, favored virus removal when compared to sand columns. They concluded that adsorption to soil mineral surfaces was responsible for the removal, and observed that filter aids, high ionic

strength (I), and coagulants enhanced removal.

Cookson and North (9,10) investigated adsorption of bacteriophage on activated carbon by kinetic and surface esterification experiments. Their work demonstrates the importance of electrostatic interactions in adsorption. Previous investigators (11) have suggested that Van der Waals interactions might be involved in virus adsorption. This investigation has shown that these interactions play a dominant role, vary markedly between different substances, and can be understood from a physical perspective.

Other investigations on virus adsorption have been extensively reviewed by Gerba et al. (11). In general, low pH (3.0 to 6.0) favors adsorption compared to high pH (8.0 to 10.0), and divalent cations favor adsorption compared to monovalent cations. Organic material may compete with viruses for adsorption sites, but in some cases, virus adsorption is still quite strong even in the presence of high concentrations of organics. For example, γ-Fe_2O_3 effectively adsorbs respiratory syncytial virus from infected egg allantoic fluids (12). Mitchell and Jannasch (13) and Smith et al. (14) show that adsorption of virus to suspended solids in seawater inhibits the rapid decrease in titer found in controls not containing solids, possibly protecting the virus from spontaneous decay. In addition, Shaub and Sagik (15) show that virions of mengo virus retain infectivity when adsorbed to bentonite. Our investigation has first demonstrated that adsorption of virus to some inorganic surfaces actually degrades the virus into small fragments.

Problems associated with potential cancer risks to man by chlorinated drinking water have only recently been recognized (16). Over 700 organic compounds have so far been detected in water (17). Chlorination of these in water treatment plants causes formation of trihalomethanes (THMs) and other halogenated substances. A significant fraction of these compounds are mutagenic (18), carcinogenic, teratogenic, and fetotoxic (17). Page et al. (17) have recently estimated potential gastrointestinal and urinary tract cancer mortalities for THMs with linear accumulated dose - animal testing models, and also with epidemiologic associations. Estimates of 20 to 300 cancer deaths annually per million population corresponded to a drinking water THM concentration of 250 ppb. This level of contamination is higher than that found in many municipal drinking water supplies, but is certainly within the range reported by EPA. EPA's report to Congress (16) also shows that THMs are far higher in chlorinated drinking water than in the same raw water supplies, indicating that chlorination is responsible for most of the THMs present. Risks imposed by other compounds produced by chlorination are not included in animal dose extrapolations, but are probably included in estimates based on epidemiologic associations.

The total adverse impact on human health and possibly the potential for environmental quality degeneration caused by chlorination of water is clearly significant.

An alternative disinfectant, ozone, has recently been shown to produce mutagens in domestic wastewater effluent (19). Adverse health effects could be implicated here as well, although this cannot be stated with certainty from Ames test results alone.

It is clear that new disinfection processes must be designed which do not increase the cancer risk of the water consumer. Discharge of chlorinated wastewater to the environment might have other long-term deleterious effects as well. It was in response to these needs that this investigation was initiated.

SECTION 2

CONCLUSIONS

Using poliovirus type 1 as a model enterovirus, it was established with a wide range of materials, that adsorption is controlled by the balance between electrostatic double layer interactions and electrodynamic Van der Waals interactions. This control was demonstrated by showing that adsorption free energies calculated from mass action arguments are in good agreement with adsorption potentials calculated from the Derjaguin-Landau-Verwey-Overbeek-Lifshitz (DLVO-Lifshitz) theory of colloid stability (20-22). Since this virus is quite characteristic of enteroviruses in terms of size--27 nm diameter, and geometry--icosahedral-spheroidal (23), electrokinetic properties of many types, and survival in the environment (24), these adsorption studies should be representative of enteroviruses in general.

The DLVO-Lifshitz theory provides us a fundamental, organized frame of reference in which to understand virus adsorption, and allows prediction of the types of materials and solution conditions conducive to virus adsorption and those that are not.

Some solids, e.g. MnO_2, CuO, and most notably, Al metal, degrade virus during adsorption. Techniques for recovering all viruses from solids that did not degrade them, e.g. Fe_2O_3, Al_2O_3, may in the future, be applicable for evaluating all virus adsorbed to other solids.

When information gained in mechanism and degradation studies was applied to a bench scale system with a 1 cm bed of Al and 0.7 min residence time, it was found that Al metal removes >99% of the input virus titer from secondary effluent at steady-state. Al metal is substantially more effective than granular activated carbon for the purpose of virus removal. It has good potential for eventual use in advanced water and wastewater treatment systems.

SECTION 3

RECOMMENDATIONS

It is recommended that future investigations of virus adsorption be centered around the following objectives:

1. DLVO-Lifshitz theory should be the framework from which future investigations of virus adsorption are conducted.

2. Investigation should continue in regards to role of conformational states on virus adsorption.

3. Competition for adsorption sites by naturally occurring organics deserves additional investigation, particularly with aluminum metal as the adsorbent.

4. Differences in adsorption characteristics of different viruses needs additional study. Adsorption and degradation of infectious hepatitis is especially important, because it is the most significant waterborne viral disease. This, of course, depends on the development of a practical assay system for hepatitis, which is currently not available.

Additional investigation should be made in regards to the use of aluminum metal as an adsorbent in an adsorption-degradation unit process. An engineering design and economic optimization study which determines how the metal might most effectively be used to provide complete virus removal at minimum cost is required prior to application in treatment plants.

SECTION 4

MATERIALS AND METHODS

VIRUS AND ASSAY

Plaque-purified poliovirus type 1, strain LSc2ab, obtained from Dr. F. L. Schaffer, Naval Biomedical Laboratories, Oakland, California, was propagated and assayed in rhinovirus adapted HeLa cells obtained from Dr. V.V. Hamparian, Medical Microbiology, Ohio State University, Columbus, Ohio.

The virus was labeled by growing it in media containing ^{3}H-uridine [5,6 ^{3}H] - 0.5 to 54 µci/ml, and ^{14}C-amino acid mixture 0.4 to 15 µci/ml, obtained from New England Nuclear, in the presence of 0.5 to 1 µg/ml actinomycin D, gift of Merck, Sharp and Dohme Research Labs. For mechanism and degradation experiments, the virus was purified of unincorporated label and cellular debris by differential ultracentrifugation, extraction with $C_2Cl_3F_3$, sucrose gradient rate zonal sedimentation, isopycnic banding in a CsCl gradient, and dialysis against saline-bicarbonate 0.02 I buffers. In degradation experiments, preparations were filtered through 0.45 µm membrane filters (Millipore Corp.) after dialysis. For process experiments, virus was labeled with mixed ^{14}C-amino acids alone and required only partial purification by $C_2Cl_3F_3$ extraction and differential ultracentrifugation.

Sucrose gradients of purified preparations showed that viruses were not clumped (25) but existed as a suspension of discrete virions. Fresh preparations were used for all experiments. When a significant decrease in the infectivity of the stock was observed, the preparation was discarded and a new one prepared. Fourteen batches were prepared for this study.

Ratios in absorbance of purified preparations at 260 to 280 nm varied from 0.91 to 1.65, slightly less than the ideal ratio (26), 1.70 ± 0.02. This indicates that if the preparations are essentially free of contaminating nucleic acids, a minor amount of protein impurity is present even after rigorous purification.

Assays were done by the monolayer method of Dulbecco and Vogt as adapted by McLain and Schwerdt (27). Cells were maintained in Eagle's minimal essential medium (MEM) with Earle's or Hanks' salts containing 400 U/ml penicillin G and 100 µg/ml streptomycin sulfate plus 10% fetal bovine serum. Media and serum were obtained from Grand Island Biol. Co. and Microbiol. Assoc. For degradation and process experiments, the penicillin concentration was reduced to 100 U/ml.

Where contamination was a severe problem, as in virus assay in the presence of secondary effluent, additional antibiotics were added to the assay overlay medium. Concentrations were: penicillin G - 1000 U/ml, streptomycin sulfate - 100 µg/ml, gentamycin sulfate - 40 µg/ml, and amphotericin B - 2.5 µg/ml. No effect of these high concentrations on titer was seen in controls.

Serial dilutions were prepared in Hanks' balanced salt solution, from Grand Island Biol. Co., plus 3.6% MEM and 0.4% fetal bovine serum. This mixture contains albumin levels adequate to block virus adsorption to dilution tubes (28,29).

Radioactivity was measured by liquid scintillation counting in a Tri - Carb model 3003 instrument with Insta Gel, both from Packard Instruments. Virus particle to PFU ratios were required for measurement of surface area coverage. Ratios were determined from plaque assays and total virus particle counts obtained from spectroscopic information, using an absorbance constant of 1.32×10^{12} particles per absorbance unit/cm. This constant was obtained from extinction coefficients given by Charney et al. (30), - a 60 subunit (isomolar with respect to structural polypeptides) model of the virion, and the polypeptide molecular weight determinations made by Maizel and Summers (31). Joklik and Darnell (32) found a constant of 1.3×10^{12} particles per absorbance-unit/cm, using a similar approach.

STATISTICS OF ASSAY DATA

Fractional standard deviations (SD) of individual plaque assay data (titer) and sample radioactivity can be estimated with the expression

$$SD = \left(m\sigma^2 + \frac{N + b}{N^2}\right)^{1/2} \qquad (1)$$

where m = total number of pipetting steps,
σ = mean standard deviation of pipetting operations,
N = number of plaques or counts taken,
b = background counts.

This expression, derived from statistical analysis presented by Wang et al. (33), assumes that the formation of plaques or counts are random events, and that pipetting variation, measured at 0.75% to 3.25%, is normally distributed. A value of 0.04 was used for σ, twice the measured mean pipetting variation, to account for increased variance attributed to non-random selection of pipettes used in preparing tubes for serial dilutions. The non-randomness is present because one pipette was commonly used to prepare as many as ten dilution tubes in sequence. Comparison of standard deviations predicted by Eq. 1 with values obtained from replicate titrations and liquid scintillation counts gave excellent agreement (34).

BUFFERS

Adsorption experiments were conducted in 1.093×10^{-2} M $NaHCO_3$ plus 9.156×10^{-3} M NaCl* (0.02 I buffer), and in 1.516×10^{-2} M $NaHCO_3$ plus 2.941×10^{-1} M NaCl (0.305 I buffer)†. Buffers were prepared in double-distilled deionized water (ddd H_2O) and equilibrated with 5% CO_2 in air to pH 7 at 15°C.

Degradation experiments were carried out in 0.02 I buffer. Sequential extractions were done with "elution media" of the following compositions:

	Normal	10x Concentrate
$NaHCO_3$	0.01 M	--
Na_2 ethylene diamine tetraacetate	0.001 M	0.01 M
Sodium dodecyl sulfate	0.2%	2%
Glycine	0.01 M	0.1 M
Bacto tryptone (Difco)	0.1 mg/ml	1 mg/ml
Fetal bovine serum	1%	10%
pH	8.8	12.0 (before dilution)
		9.8 (after dilution)

The 10x concentrate produced a medium almost identical to normal elution medium when diluted 1:10 with 0.02 I buffer. All buffers except those used in process experiments were sterilized by 0.22 μm membrane filtration.

Process experiments also used composite unchlorinated secondary effluent from the Palo Alto wastewater treatment plant.

ADSORBENTS

Adsorbents selected for study were non-porous α-SiO_2, α-Fe_2O_3, β-MnO_2, CuO, α-Al_2O_3, Si metal and Al metal. This group of materials has a wide range of dielectric, electrokinetic, and chemical properties for assistance in resolving the adsorption mechanism. Because many of these materials are common in nature, adsorption information on these solids should be relevant in an environmental context.

The SiO_2, Min·U·Sil 5 powder, gift of Pennsylvania Glass Sand Corp., was cleaned by repeated overnight refluxing in aqua regia, 16 M HNO_3, and then by

*Some buffers were accidentally prepared with 1% less NaCl in adsorption mechanism studies.

†Buffer compositions were determined by chemical titrations and equilibrium calculations including activity corrections and complexation (34).

rinsing in ddd H_2O between and after refluxing. Refluxing in acid was continued $\geq$ 5 times until analysis of the supernatant showed that additional refluxing would remove little of the remaining iron impurity. The SiO_2 used in process experiments was Extra Fine Jasper, 0.03 to 0.08 mm in diameter, likewise a gift of Pennsylvania Glass Sand Corp. It was washed extensively in deionized water to remove particles < 0.03 mm in diameter and cleaned as described above. It was rinsed in dilute NaOH prior to acid refluxing to help disperse adhering particles.

Fe_2O_3, MnO_2, and CuO powders were ACS reagent grade materials aged for 14 days at 90-95°C and washed extensively with ddd H_2O to remove finer particulates. Al_2O_3, Linde A alumina powder, manufactured by Union Carbide, New York, N.Y., was obtained from Dr. R.L. Bassett, U.S. Geological Survey, Menlo Park, California. It was aged overnight in ddd H_2O at 25°C and rinsed once in ddd H_2O prior to use. Silicon metal semiconductor wafers, 30 ohm-cm N and 0.3 ohm-cm P types, were manufactured by Monsanto Chemical Company, St. Louis, Missouri. Aluminum metal was ACS reagent powder or metal foil, obtained from Reynolds Metals Corp. Aluminum metal was cleaned by rinsing in dilute NaOH and HCl, and ddd H_2O.

Oxide structural forms were confirmed by x-ray diffraction. Greek letters α, β, and γ, refer to structural forms. The oxides and Al powder were sterilized by heating to 200° C for $\geq$ 2 hr, and were stored dry. Si metal was sterilized by overnight exposure to high intensity UV ($\sim 10^4$ erg/cm^2 sec).

The solids CuO, Al metal, Al_2O_3, and Si metal, are thermodynamically unstable for the given reaction conditions in adsorption-desorption experiments. The stable phases are malachite, $Cu_2(OH)_2CO_3$ (35), γ-Al_2O_3 (36,37), and α-SiO_2 (37), respectively. The surfaces of these materials may well be altered to the stable phase during experiments, except for Si metal, where the oxidation is known to be kinetically limited, the surface phase altering instead to amorphous silica (38).

Clay minerals were not selected because they have at least three types of sites, plate, edge, and interlayer, which would substantially complicate analysis of adsorption information.

CHEMICALS, ISOTOPES, AND ANALYTICAL METHODOLOGY

Chemicals used during this study were ACS reagent or higher quality material unless specified otherwise. ^3H_2O solutions for use in process experiments were purchased from New England Nuclear.

In plaque assays, scintillation counting, and coliform assays, standards were always analyzed concurrently with samples. Data from these samples were compared only to standards run in parallel. Occasionally samples required retitration by plaque assay. If standards run in parallel during both assays were comparable, data obtained by retitration were accepted. If not, the data point was discarded or the experiment repeated.

COD, suspended solids, and total coliform (membrane filter) determinations conformed to procedures listed in Standard Methods for the Examination of Water and Wastewater (39).

SECTION 5

MECHANISM OF POLIOVIRUS ADSORPTION

THERMODYNAMIC APPROACH

The purpose of this section is to evaluate the mechanisms by which enteric viruses adsorb to representative inorganic surfaces, using poliovirus type 1, strain LSc2ab as the model virus.

The overall free energy of an adsorption process (ΔG_{ads}) can be broken down into various components,

$$\Delta G_{ads} = \Delta G_{dl} + \Delta G_{VdW} + \Delta G_{hyd} + \Delta G_{cov\text{-}ion} \cdots - T\Delta S_o \qquad (2)$$

each of which arises from a different type of interaction. The subscripts dl, VdW, hyd, and cov-ion refer to energy contributions that come from the interaction of double layers, Van der Waals potentials, surface hydration, and covalent-ionic interactions respectively. T is the absolute temperature, and ΔS_o represents entropy changes not accounted for in other terms.

The approach has been to evaluate the overall ΔG_{ads} and then to compare these values to values of the components calculated from theory, where possible. Terms not possible to evaluate analytically are examined by critical hypothesis-and-test experiment or by comparison to their importance in analogous systems.

DETERMINATION OF ΔG_{ads}

Mass Action Equation of State

The overall free energy of adsorption can be determined with the mass action equation of state derived by Dhar *et al.* (40),

$$\frac{\theta}{x(1-\theta)^x} = \frac{C_{eq}}{C_{H_2O}} \exp\left(\frac{-\Delta G_{ads}}{RT}\right) \qquad (3)$$

where C_{eq} = molality of adsorbate, solution phase

C_{H_2O} = molality of H_2O

R = gas constant
T = absolute temperature in degrees Kelvin
θ = fraction of surface covered by adsorbate
x = relative size factor; molecules of solute desorbed per molecule adsorbate adsorbed.

Evaluation of valid free energies from this equation requires determination of the variables C_{eq}, C_{H_2O}, θ, and x, and establishing that the system is reversible and at equilibrium. The variables C_{eq} and θ are determined from adsorption-desorption isotherms, i.e., C_{eq} versus θ plots, measured with plaque assay data in conjunction with virus particle to PFU ratios, space filling models of the virus structure, and measured surface areas of the adsorbents. The relative size factor x, estimated to be ~50, is obtained from space filling models as well, assuming ~3 percent of a virion face will approach a surface closely enough to displace one water molecule.

A temperature of 15° C was chosen for free energy determinations because it is characteristic of the average natural water temperatures in temperate climates.

If adsorption and desorption data points for a given isotherm coincide within the normal range of data scatter, then conditions required for determination of ΔG_{ads} of the adsorption reaction, that is equilibrium and reversibility, are met. This approach is far better than simply following the course of adsorption experiment with time, because it evaluates both equilibrium and reversibility criteria simultaneously.

Adsorption-Desorption Experiments

Adsorption-desorption experiments on oxides and Al powder were done in sterile 15 ml screw-capped borosilicate glass tubes, covered with flamed alumimun foil to prevent leakage. Procedures for the experiments are listed below in sequence.

1. Addition of the solid phase, 0.02 to 3 g, depending on the solid, to the reaction vessel, weighing before and after addition.

2. Rinsing the solid twice with the same type of buffer used in adsorption to eliminate possible shifts in buffer composition due to double layer formation on the solid. For experiments with CuO, MnO_2, and Fe_2O_3, buffers were pre-equilibrated $\geq$ 4 hr with the respective solid phases. Centrifugation at 1000g for 10 min in an IEC PR-2 refrigerated centrifuge was used for solid-liquid separation.

3. Addition of 10 ml of buffer to the reaction and resuspending solids with a vortex mixer.

4. Addition of virus 10^5 to 10^8 PFU with micropipette.

5. Adsorption of virus during slow rotation (0.5 or 1 RPM) for 2 hr in a rotator mounted in a 15°C incubator. In addition to slow rotation,

samples were shaken by hand at 30 min intervals to insure good mixing.

6. Centrifugation of tubes as described in step 2 and sampling for residual infectivity and radioactivity. The buffer was then aspirated and the reaction vessels weighed to determine the quantity of residual buffer left around the solid.

7. Addition of 10 ml of buffer, not containing virus, to the reaction vessel and replacement of flamed foil cap. Solids were then resuspended gently with a vortex mixer.

8. Desorption of virus into "clean" buffer during slow rotation for 2 hr, shaking at 30 min intervals as described in step 5.

9. Centrifugation, as in steps 2 and 6, followed by sampling the supernatant for determination of the equilibrium concentrations of virus for the desorption step.

In adsorption-desorption experiments with SiO_2 an additional step of centrifugation for 10 min at 15,000g in the 40.2 rotor of a Spinco Model L ultracentrifuge from Beckman Instruments was required for complete solid-liquid separation on aliquots withdrawn from the reaction vessel for assay.

Adsorption experiments on aluminum foil were done in T-25 tissue culture flasks from Corning Glass Works. Experiments were done in an identical manner as those described above, except that they were placed on a sample oscillator, which gently rocked the samples at 1.5 Hz.

The reaction times for both the adsorption and desorption steps were increased to 10 hr, and centrifugation was not required for solid-liquid separation.

Adsorption-desorption experiments on Si metal were done in Corning 60 x 15 mm polystyrene, tissue-culture petri dishes to which the Si chips had been attached with polystyrene cement. Experiments were done as described with Al foil, except that the reaction time was decreased to 4 hr for both the adsorption and desorption steps and petri dishes were placed on the oscillator in a sealed container with an atmosphere of 5% CO_2 in air to keep the pH constant. The apparatus is shown in Figure 1.

Controls demonstrated that rotation and oscillation during the experiments and dissolution products of the adsorbents had no significant effect on virus titers with 5 hr incubation times, and that adsorption to reaction vessel surfaces was statistically insignificant.

Radioactivity adsorption data corresponded to infectivity adsorption data for SiO_2 and Si metal, the weakest adsorbents. On other materials, however, more radioactivity was present in the equilibrium supernatants than infectivity, even though both were reduced to exceptionally low levels. Because purified preparations contain minor amounts of impurity and degradation products, which cannot be avoided, this discrepancy may be due to

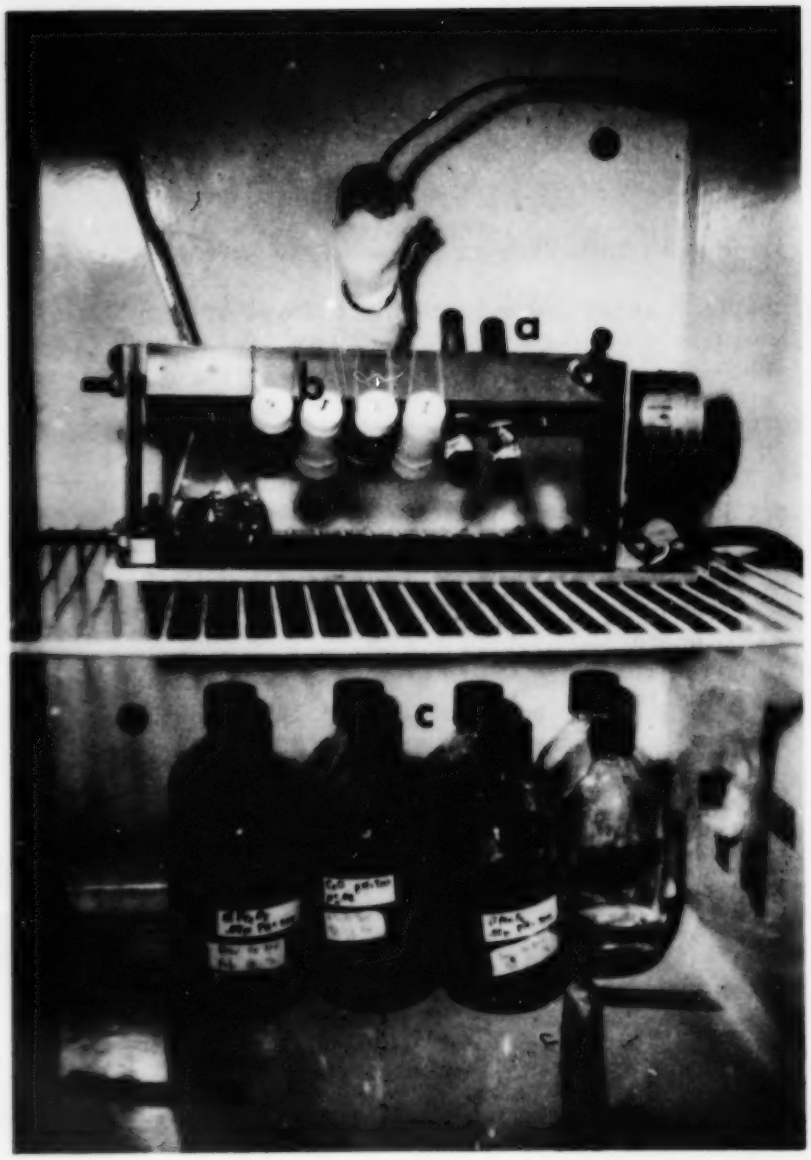

Figure 1. Adsorption (a) and degradation (b) apparatus. Buffers for experiments with transition metal oxides were pre-equilibrated with respective solid phases (c).

preferential adsorption of virus compared to impurity. Except for one data point on SiO_2 at 0.02 I, infectivity data and particle to PFU ratios were used to construct adsorption isotherms in all cases.

Surface Area Determinations

Specific surface area determinations were required for the calculation of θ, the fraction of available surface covered by virus particles at equilibrium. BET theory (41) and N_2 adsorption at 77.5°K to 77.6°K were used where feasible, to determine surface area, assuming a molecular site occupancy of 16.2 A^2. Adsorption data were obtained with an Orr Model 2100 instrument manufactured by Micromeritics Instruments Corp. Results are presented in Table 1. Accuracy of ±20% is suggested by Jura (42). The BET value we obtained for Min·U·Sil 5 is quite consistent with results obtained by other investigators, (e.g., 43,44).

These BET values are compared to surface areas obtained from Kozeny air permeability methods (45) as a check on validity. A 0.39 m^2/g (BET-Kr) standard, obtained from Dr. G.A. Parks, Applied Earth Sciences, Stanford University, was used to calibrate the Kozeny instrument. Kozeny values are also presented in Table 1.

According to the discussion of Jura (42) and Schultz (46) these two methods of surface area determination are not directly comparable. BET surface areas are considered most accurate (42) and these have been selected for calculating θ where available. Kozeny methods (46) measure only surface in a packed column that is adjacent to air flow paths, and which could be expected to give smaller areas than BET methods.

The BET surface area of Al metal powder was estimated from the Kozeny value times the average BET:Kozeny ratio (3.5 ± 1.6) for other samples. On Al foil and Si (monocrystalline) semiconductor chips, the surface areas were estimated by direct measurement times a roughness factor of two, estimated from geometric considerations of etched metallic surfaces.

Adsorption Isotherms and ΔG_{ads}

Having obtained adsorption-desorption data and specific surface areas, data were assembled as isotherms.

Adsorption-desorption isotherm data were calculated with the following equations:

$$C_{eq} = \frac{\text{PFU/ml}_{1,2} \times \text{PPR} \times 10^3 \text{ g/kg}}{N_a \times \rho} \qquad (4)$$

TABLE 1. SURFACE AREAS OF ADSORBENTS

Solid	BET-m^2/g	Kozeny - m^2/g (duplicates)
α-SiO_2*	3.95 ± 0.79	1.43, 1.44
α-Fe_2O_3	2.33 ± 0.47	0.61, 0.79
β-MnO_2	0.38 ± 0.08	0.11, 0.10
CuO	0.29 ± 0.06	0.16, 0.16
α-Al_2O_3	14.6 ± 2.9†	2.38, 2.34
Al Powder	(0.13)‡	0.037, 0.038
Al Foil#	0.0012 m^2/g	ND§
Si Metal#	0.0039 m^2	ND

*BET surface area of SiO_2 used in degradation experiments was 5.49 ± 1.10 m^2/g.
†Determination by Dr. R. L. Bassett, U.S. Geol. Survey.
‡Estimated from average BET:Kozeny ratio found with other samples.
§Not determined.
#Areas obtained by direct measurement times a roughness factor of two.

and

$$\theta = \frac{Ads_{1,2} \times PPR}{w_a \times S_a \times PI} \tag{5}$$

where Ads_1 = Tot - $PFU/ml_1 \times V_a$ (6)

Ads_2 = $Ads_1 + PFU/ml_1 \times V_r - PFU/ml_2 \times V_d$ (7)

and $PFU/ml_{1,2}$ = plaque forming units per ml. Subscript 1 refers to adsorption supernatants, subscript 2 refers to desorption supernatants.

PPR = particle to PFU ratio,
PI = packing index, 1.58×10^{15} virion sites per m^2 (34),
ρ = buffer density,

N_a = Avogadro's number,

w_a = weight of adsorbent,

S_a = specific surface area,

$Ads_{1,2}$ = virus adsorbed to solid,

Tot = total virus initially added,

V_a = volume of buffer during adsorption,

V_r = volume of buffer remaining after aspiration,

V_d = volume during desorption.

The subscripts 1 and 2 in these expressions refer to adsorption and desorption steps, respectively.

Isotherms determined on SiO_2, Fe_2O_3, MnO_2, and CuO, determined at 0.02 and 0.305 ionic strength, are presented in Figures 2 and 3, respectively. Isotherms determined on Al_2O_3 and Al metal, at an ionic strength of 0.02, are presented in Figure 4. Isotherms were fit by linear regression analysis of log:log plots with 1:1 slopes appropriate for low values of θ. A log C_{eq} value of -17 corresponds to approximately 5 PFU/ml, a value of -11 corresponds to approximately 5 x 10^6 PFU/ml. Approximate nature of correspondence is related to variation in virus particle to PFU ratios among preparations.

On Si metal, we could estimate only a limiting value, because the amount which appeared to be adsorbed ($Ads_{1,2}$) was within the statistical precision of the individual assays.

Where adsorption and desorption data points coincide, within the normal range of data scatter, isotherms appear to be reversible and to approach equilibrium. This was found to be the case on all materials except on Al metal and on CuO at high ionic strength, where the reactions were clearly irreversible. For these two cases, on the desorption step, in all samples except one - where we counted one plaque, data points were below detection limits of routine plaque assay procedures.

At low surface coverage, where $(1-\theta)^X \rightarrow 1$, the reversible reactions are linear, within the normal range of data scatter. The apparent linearity and reversibility of these reactions suggest that the interaction energy between virus and adsorbent does not change substantially as a function of the location on the surface where adsorption takes place.

Adsorption free energies, calculated from Eq. 3, are listed in Table 2. The values were obtained by linear regressions with 1:1 slopes at a θ of 10^{-5}. Standard deviations are based on data scatter about the regressions.

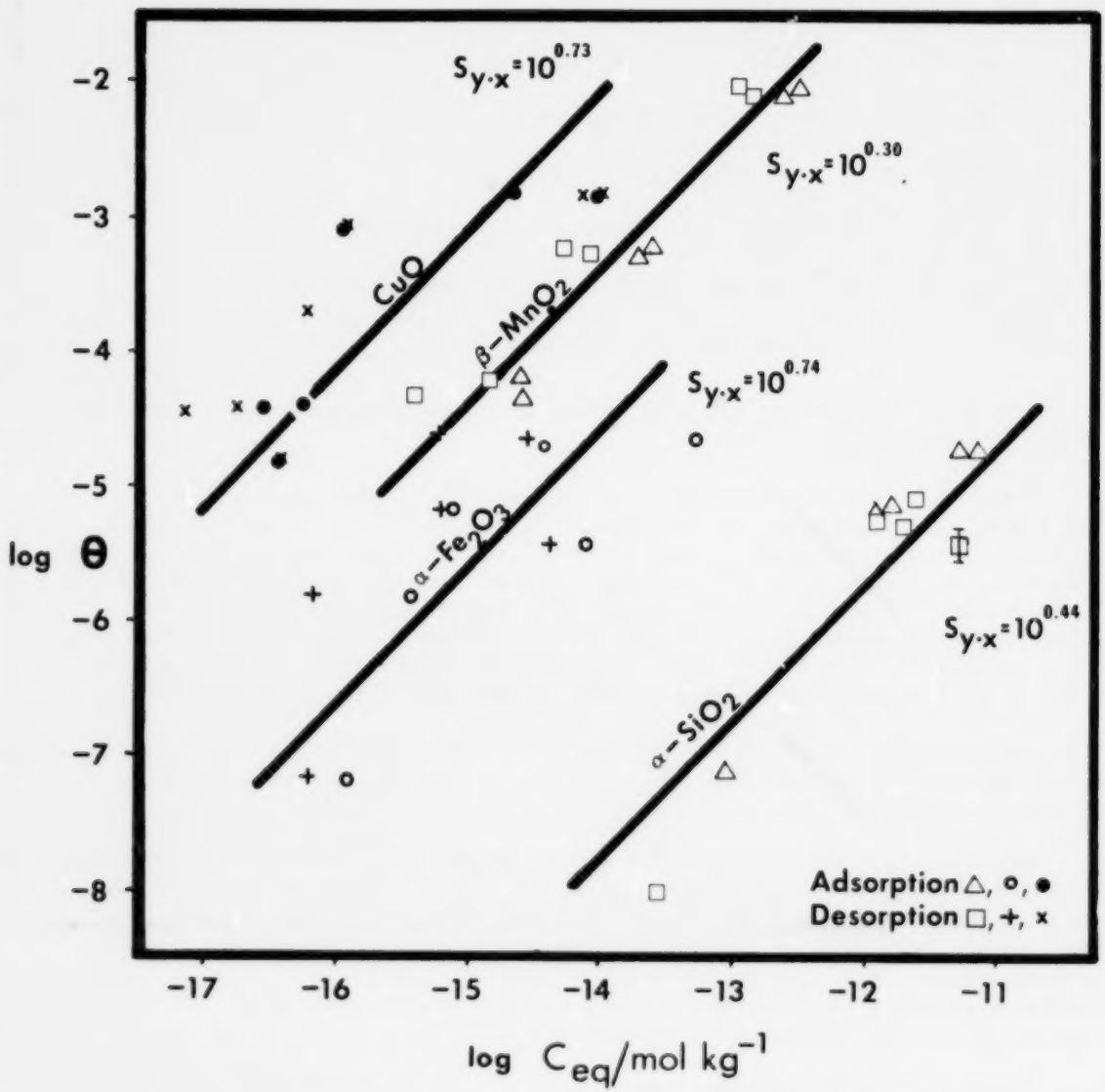

Figure 2. Adsorption-desorption isotherms of poliovirus on oxides at 0.02 ionic strength and pH 7. θ is the fraction of surface covered, C_{eq} is the equilibrium virus concentration (mol/kg) in solution. Sy•x is the standard deviation (n-2 degrees of statistical freedom) of log θ about regression lines. The error bar represents theoretical precision of plaque assay data.

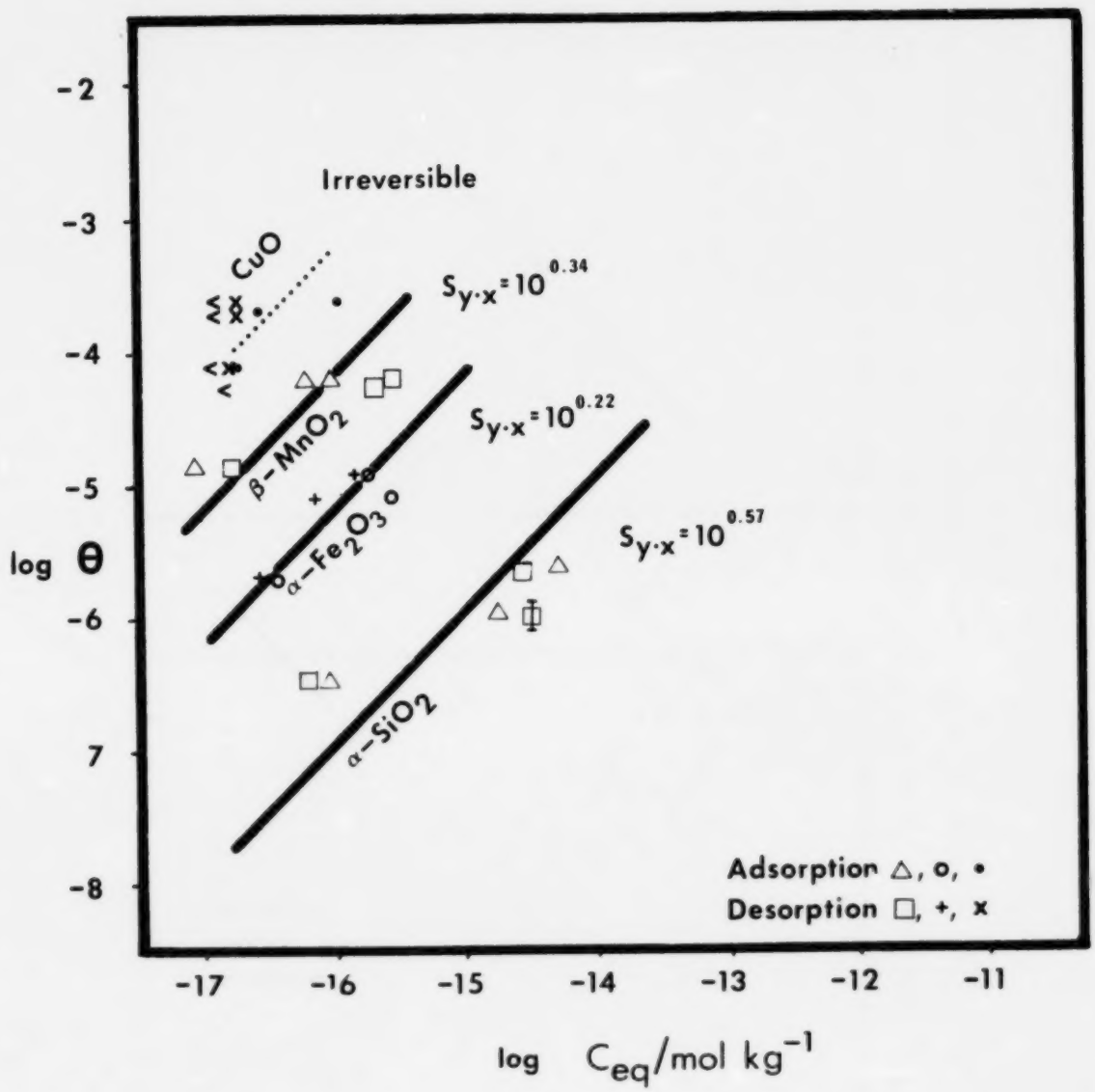

Figure 3. Adsorption-desorption isotherms of poliovirus on oxides at 0.305 ionic strength and pH 7. The error bar represents theoretical assay precision. < designations refer to points below detection limits of the assay system, corresponding to <8 PFU/ml.

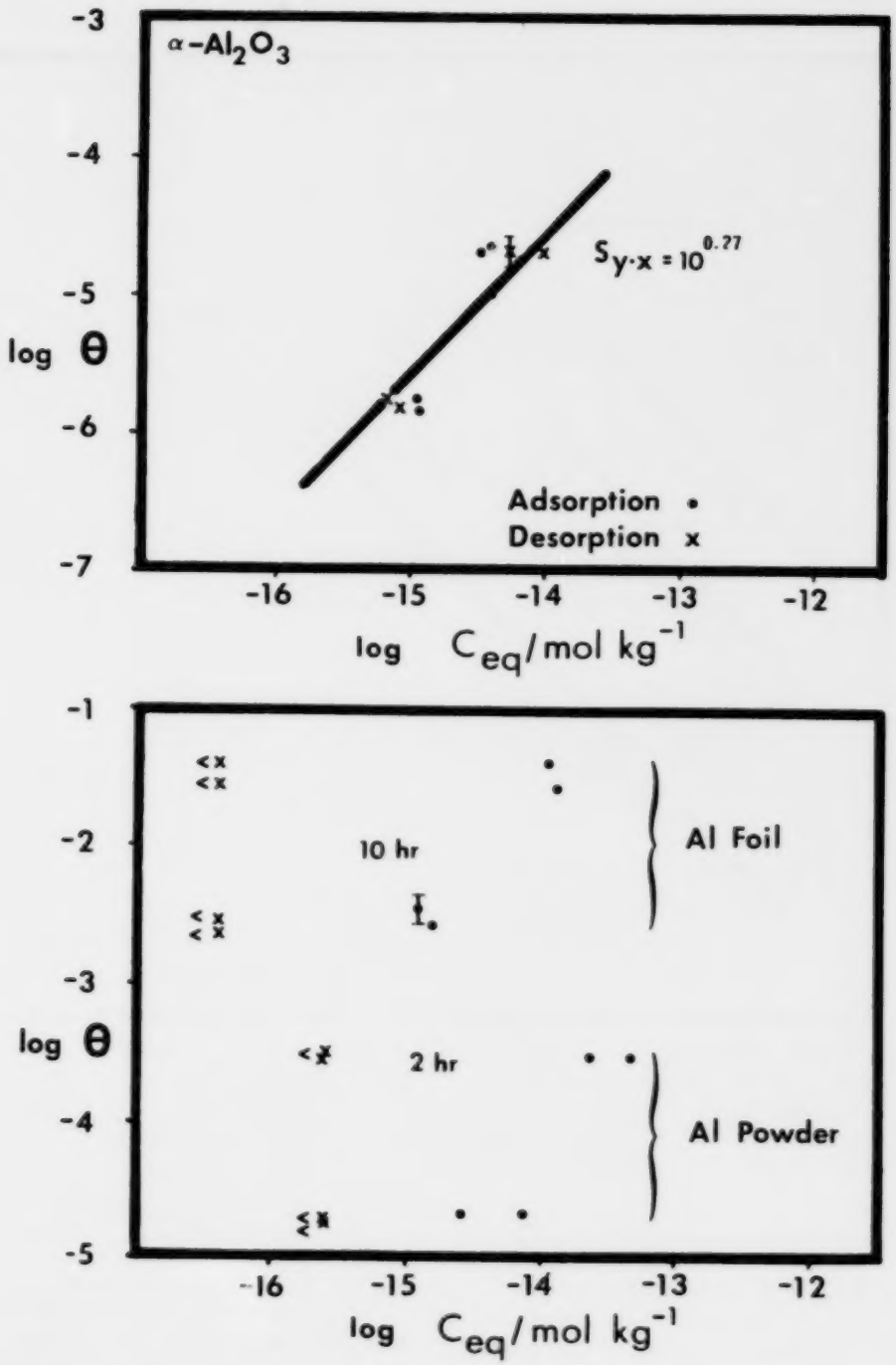

Figure 4. Adsorption-desorption isotherms of poliovirus on Al_2O_3 and Al metal at 0.02 ionic strength and pH 7. < designates points below detection limit.

TABLE 2. FREE ENERGIES OF POLIOVIRUS ADSORPTION ON OXIDE SURFACES AS DETERMINED BY MASS-ACTION EQUILIBRIA

Solid	ΔG_{ads} - kJ/mol 0.02 I	ΔG_{ads} - kJ/mol 0.305 I
α-SiO_2	-32.4 ± 2.4	-50.0 ± 3.1
α-Fe_2O_3	-52.9 ± 4.0	-59.9 ± 1.2
β-MnO_2*	-58.9 ± 1.7	-65.3 ± 2.1
CuO*	-65.8 ± 4.0	Strong†
α-Al_2O_3	-52.3 ± 1.5	ND#
Al Metal	Very Strong†	ND
Si Metal	≥ - 39.5	ND

*These calculated values may be 4 to 9 kJ/mol too negative on the basis of our degradation studies.
†Irreversible reactions.
#Not determined.

Actually, as presented in the next major section of this report, virus is degraded by adsorption on some surfaces, notably MnO_2, CuO, and Al metal. In these cases, we estimate that our free energies as listed may be 4 to 9 kJ/mol too negative. This degree of error is only twice the normal range of data scatter about the isotherms. It does not change the free energy values enough to alter the purpose to which these free energies are put, that is, evaluation of the adsorption mechanisms.

Because it is rather difficult to visualize the differences in effectiveness of these solids as adsorbents from free energy data, expected equilibrium titers on these materials were calculated assuming a PPR of 10^3, 25°C, a θ of 10^{-5}, and have been listed in Table 3. This normalizes all system variables except the chemical nature of the solid phase. In terms of equilibrium titer, there is at least 5 orders of magnitude difference between the effectiveness of the strongest and weakest adsorbents.

APPLICATION OF DLVO-LIFSHITZ THEORY

The approach in evaluating the contributions from double layer interactions and Van der Waals interactions according to the DLVO-Lifshitz theory, was to compare differences in ΔG_{ads} with differences in potentials (U) evaluated theoretically. In evaluating the potentials, as detailed later, a highly complex interaction of a spheroidal-icosahedral, deformable virus with a real surface has been approximated with a sphere-plate model. To adjust for errors introduced by this approximation, characteristic separation distances in the models between virus and solid were taken to be adjustable parameters. Because

TABLE 3. NORMALIZED CONCENTRATION OF POLIOVIRUS INFECTIVITY IN EQUILIBRIUM WITH VARIOUS SOLIDS

Solid Phase	Equilibrium Virus Titer log PFU/ml 0.02 I	0.305 I
α-SiO_2	7.15 ± 0.43	4.07 ± 0.55
α-Fe_2O_3	3.56 ± 0.71	2.34 ± 0.21
β-MnO_2	2.50 ± 0.29	1.39 ± 0.36
CuO*	1.30 ± 0.71	→ $-\infty$
α-Al_2O_3	3.66 ± 0.26	ND
Al Metal*	→ $-\infty$	ND
Si Metal	≥ 5.90	ND

*Includes significant amount of degradation as well as adsorption.

assumptions in double layer models and Van der Waals models are different, values for characteristic separations are not expected to be the same.

The test of the comparison of differences in ΔG_{ads} and U are then two-fold: (1) do potentials match free energies for all solid tested, (2) are values selected for characteristic separation distances realistic regarding current understanding of the molecular structure of solid-liquid interfaces, i.e., 0.1 to 1 nm. If these two considerations are met, we have good evidence that DLVO-Lifshitz theory explains virus adsorption on solids tested.

ELECTROSTATIC COMPONENTS OF ΔG_{ads}

A major contribution to the free energy of adsorption comes from the interaction of double layers that form about the virus and solid phases. Double layers exhibit localized concentration excesses of either negative or positive ions adjacent to charged surfaces in solution.

Viruses and oxides are thought to develop charged surfaces in solution by ionization of prototropic groups on their surfaces (47). Current treatment of double layers show at least two principle regions, the inner or Stern layer and the outer or Gouy layer. These are shown diagrammatically in Figure 5.

When double layers from different particles interact, they develop repulsive or attractive forces depending on whether they are of like or opposite electrical charge. Integration of these forces over distance from large distances of separation until the particles collide will give potential energy values which can evaluate double layer contributions to the ΔG_{ads}.

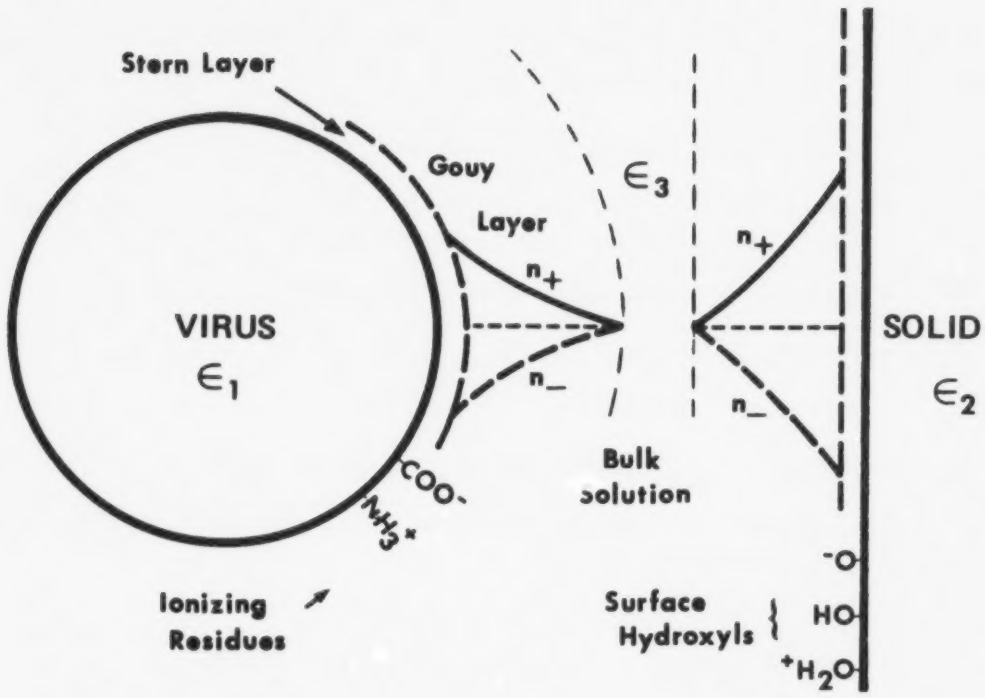

Figure 5. Diagrammatic representation of double layers about virus and solid. The presentation shows ionizing residues and surface hydroxyl groups thought responsible for charge development; the Stern layer of bound cations, anions, and water molecules; and the Gouy layer with cation (n_+) excesses and anion (n_-) deficits. ϵ_1, ϵ_3, and ϵ_2 are the complex dielectric susceptibility functions important in controlling the differences in magnitudes of Van der Waals interactions with different materials.

We have used the constant charge LSA* expression derived by Gregory (48) for sphere-plate boundary conditions

$$U_{dl} = N_a\ 128\ \frac{(a_v + 0.5\text{nm})\ \pi n k_B T}{\kappa^2}\ \gamma_1\gamma_2\ \exp(-\kappa\ d_{es}) \qquad (8)$$

where U_{dl} = double layer interaction potential per mole,

a_v = virion radius - 13.5 nm; 0.5 nm is added to account for Stern layer thickness according to Smith (49),

n = anion or cation density (per m^3) in solution,

N_a = Avogadro's number,

k_B = Boltzmann's constant,

κ = $(2e^2nz^2\ /\ \varepsilon_o\varepsilon_v\ k_BT)^{\frac{1}{2}}$, the Debye inverse length,

ε_o = relative dielectric constant of immersion medium at zero frequency,

ε_v = dielectric permittivity of free space,

$\gamma_{1,2}$ = $\tanh\ (y_{1,2}/4)$

$y_{1,2}$ = $ze\psi_{1,2}\ /k_BT$,

z = charges per ion,

e = electronic charge,

$\psi_{1,2}$ = Gouy Chapman surface potential,

d_{es} = interaction separation distance for electrostatic potential.

This expression predicts potentials which are intermediate between those predicted by exact constant surface potential and exact constant charge expressions. A similar intermediacy is observed with experimental data pertaining to the adhesion force of polystyrene latex particles on cellophane (50).

The only experimental data required to compute values of U_{dl} for a given system for sphere-plate boundary conditions are measured values of surface potentials $\psi_{1,2}$ for the interacting particles under a given set of experimental conditions, and the characteristic distance between them in the adsorbed

---

* Linear superposition assumption.

state. On the basis of Smith's work on oxide electrokinetics, it was assumed that $\psi_{1,2}$ were approximately equal to zeta potentials ($\zeta_{1,2}$) measured by electrophoresis experiments. A characteristic separation distance d_{es} here was assumed to be zero at coincidence of the Stern surfaces. This corresponds to a value of 1 nm between effective virus and substrate surfaces (49).

Zeta Potential Determinations for Oxides

Zeta potentials of the oxides were determined by conventional microelectrophoresis with a Zeta-Meter, manufactured by Zeta-Meter, Inc.

Electrophoretic mobilities were measured in 0.02 I buffers under conditions closely paralleling virus adsorption-desorption experiments. Zeta potentials were then calculated with the Smoluchowski equation (51). In 0.305 I buffers, the ionic strength was too high to permit accurate measurement. Zeta potentials were estimated from values measured at 0.02 I using Hunter and Wright's correlation (52)*. Values are given in Table 4.

Zeta Potential of Poliovirus

The virus zeta potentials were measured by zonal electrophoresis in a RNAse-free sucrose gradient, and an extension of the retarded, relaxed Smoluchowski equation (34,53). This extension allows correction for variation of viscosity with distance in the gradient. Again, the value of ζ at 0.305 I is estimated by applying Hunter and Wright's correlation. Values are included in Table 4.

Correspondence of Theoretical Isoelectric Points with Reported Values

As a check on the validity of the virus zeta potential measurements and to determine whether or not this strain of virus is electrokinetically similar to other enterovirus types, isoelectric points of the virus were estimated from zeta potential information and compared to reported values obtained by isoelectric focusing.

Estimates were obtained by first extrapolating the counterion concentration in Hunter and Wright's correlation to 10^{-6} M for a value of the surface potential (ψ_o). Estimates using this procedure are quite close to values obtained by Hunter and Wright (52) using more involved methods. Then the pH at which the virus has zero charge (pH_{PZC}) was calculated with the Nernst equation (47)

$$\psi_o = 2.303 \frac{RT}{F} (pH_{PZC} - pH) \qquad (9)$$

* Hunter and Wright (52) found for oxide surfaces that the measured zeta potentials plot approximately linearly as a function of the logarithm of counterion concentration and the ζ=0 intercept corresponds to a counterion concentration of ~1 M.

TABLE 4. ZETA POTENTIALS (mv) OF OXIDES AND VIRUS IN pH 7 $NaHCO_3$-NaCl SOLUTIONS

	0.02 I	0.305 I*
α-SiO_2	-44.5 ± 8.5†	-13.4 ± 2.6
α-Fe_2O_3	-28.8 ± 2.5	-8.7 ± 0.8
β-MnO_2	-20.7 ± 5.9	-6.2 ± 1.8
CuO	-17.6 ± 6.1	-5.3 ± 1.8
Poliovirus 1 LSc2ab	-5.9 ± 0.9	-1.8 ± 0.3

*Estimated with Hunter and Wright's (52) correlation.
†Values are standard deviations.

where F is Faraday's constant and pH is the pH of the solution in which electrophoresis was done. Data required for more accurate evaluation procedures, e.g. the Yates et al. model (54), are not yet available for viruses. The pH_{PZC} should be approximately equal to an isoelectric point in the absence of strong binding of ions in solution.

Comparison of estimates with reported values is presented in Table 5. Values appear to be in good agreement with those of other types (55-59).

Mandel (56) found that infectious poliovirus exists in two conformational states, A and B, each of which has a different isoelectric point. Virus that had been inactivated appeared to have an isoelectric point similar to what was measured for B state virus. There was a small amount of inactivated material (Table 5) in one of our experiments that agrees with Mandel's findings.

Mandel's conformational bimodalism has been found with many different types of enteroviruses, and should play a major role in governing adsorption of viruses to materials in the environment.

Double-Layer Interaction Potential Evaluation

Having obtained estimates of the zeta potentials of oxides and virus for the adsorption reactions, Eq.(8) can be used to evaluate double-layer interaction potentials. These are presented in Table 6 and are repulsive in all cases.

To evaluate the degree to which the adsorption-free energy is controlled by double-layer interactions, differences in the ΔG_{ads} and U_{dl} at two ionic strengths were compared. This comparison, shown in Table 7, gives excellent agreement.

TABLE 5. COMPARISON OF THEORETICAL ISOELECTRIC POINTS WITH VALUES REPORTED FOR OTHER ENTEROVIRUSES

Virus	State	Isoelectric Point	Reference
Poliovirus 1	A	6.6	
LSc2ab	non-infect.* mat.	≤ 5.7	This study
Poliovirus 1	A	7.4	(55)
Brunenders	B	3.8	
Poliovirus 1†	A	7.0	(56)
Brunhilde	B	4.5	
Poliovirus 1	A	7.5	(57)
CHAT	B	4.5	
Poliovirus 1	A	8.5 ± 0.1	(58)
Mahoney	B	?	
Poliovirus 2	A	6.5	‡
Sabin T2	B	4.5	
Coxsackievirus	A	6.1	‡
A21	B	4.8	
Echovirus 1	A?	5.6	(59)
Farouk	B	5.1	

*The Nernst method of estimating pH_{IEP} should give an overestimate if the electrophoresis pH is far from the isoelectric point (54).
†Mandel found essentially identical results with zonal electrophoresis as a function of pH as with isoelectric focusing.
‡B.D. Korant and K. Lonberg-Holm, personal communication (1977).

TABLE 6. DOUBLE-LAYER INTERACTION POTENTIALS BETWEEN VIRUS AND SOLID PHASES ACCORDING TO THE LSA EXPRESSION

Solid	U_{dl}(0.02 I) - kJ/mol	U_{dl}(0.305 I) - kJ/mol
α-SiO_2	18.9 ± 4.8*	1.9 ± 0.5
α-Fe_2O_3	12.7 ± 2.2	1.2 ± 0.2
β-MnO_2	9.2 ± 3.0	0.9 ± 0.3
CuO	7.9 ± 3.0	0.7 ± 0.3

* ± values are standard deviations.

TABLE 7. COMPARISON OF DIFFERENCES IN ΔG_{ads} and U_{dl} at 0.02 I and 0.305 I

Solid	ΔG_{ads} (0.02 I - 0.305 I) - kJ/mol	U_{dl} (0.02 I - 0.305 I) -kJ/mol
α-SiO_2	17.6 ± 4.0	17.0 ± 4.8*
α-Fe_2O_3	7.0 ± 4.3	11.5 ± 2.2
β-MnO_2	6.3 ± 2.6	8.4 ± 3.0
CuO	†	7.2 ± 3.0

* ± values are standard deviations.
† Cannot be determined because the isotherm at 0.305 I is irreversible.

ELECTRODYNAMIC COMPONENTS OF ΔG_{ads}

It is apparent that the virus is quite strongly adsorbed in spite of the repulsive nature of all mineral-virus double layer interaction potentials studied so far. The electrostatic interactions are weak where adsorption is strong and are strong where adsorption is weak. This suggests that other strong attractive forces must be involved in adsorption.

Colloid stability and polymer adsorption theory (60) suggest that Van der Waals interactions should be of major importance in systems involving interaction of particles of virus size.

Evaluation of Van der Waals interactions was made with a combined Lifshitz-Hamaker approach. Van der Waals interactions are a result of electromagnetic fields generated from dipole oscillators in one material, i.e. electronic oscillations about nuclei of constituent atoms and vibrations or rotations of molecular structures containing separated electrical charges, interacting with dipole oscillators in an adjacent material. If there is an intervening material, e.g. an aqueous solution, interacting electromagnetic fields are screened by dipoles in the immersion medium.

Dzyaloshinski, Lifshitz, and Pitaevski (22) developed a general theory of Van der Waals interactions (the Lifshitz theory) from continuum quantum field electrodynamic considerations. At small separations, < 5 nm, and at zero temperature (°K) the electrodynamic induction force (F_{132}) between two materials, designated by subscripts 1 and 2, immersed in a third medium, designated by subscript 3, according to Dzyaloshinski et al. (22), is

$$F_{132} = \frac{\hbar'}{16\pi^2 d_{ed}^3} \int_0^\infty \int_0^\infty \chi^2 \left[\frac{(\varepsilon_1 + \varepsilon_3)(\varepsilon_2 + \varepsilon_3)}{(\varepsilon_1 - \varepsilon_3)(\varepsilon_2 - \varepsilon_3)} \exp \chi - 1 \right]^{-1} d\xi \, d\chi \qquad (10)$$

where

$\hbar'$ = Planck's constant $h/2\pi$,

d_{ed} = interaction separation distance,

χ = integration variable (22),

$\varepsilon_{1,2,3}$ = complex dielectric susceptibility functions: $\varepsilon = \varepsilon'(\omega) + i\varepsilon''(\omega)$, as a function of the complex frequency $\omega = \omega_R + i\xi$.

Evaluating the integral and describing the dielectric susceptibility as a function of the imaginary frequency component (22) gives

$$F_{132} = \frac{\hbar'}{8\pi^2 d_{ed}^3} \bar{\omega}_{132} \qquad (11)$$

where

$$\bar{\omega}_{132} = \int_0^\infty \frac{[\varepsilon_1(i\xi) - \varepsilon_3(i\xi)]}{[\varepsilon_1(i\xi) + \varepsilon_3(i\xi)]} \frac{[\varepsilon_2(i\xi) - \varepsilon_3(i\xi)]}{[\varepsilon_2(i\xi) + \varepsilon_3(i\xi)]} \, d\xi. \qquad (12)$$

Describing the dielectric susceptibility as a function of the imaginary component of the complex frequency allows ready interpolation between ε values measured at different frequencies by capacitance bridge measurements or spectroscopic information (61).

The Lifshitz function is of the same form as older pairwise summation equations derived by Hamaker for plate-plate geometries

$$F_{132} = \frac{A_{132}}{6\pi d_{ed}} \qquad (13)$$

The complex Hamaker coefficient A_{132}, is related (22) to the Lifshitz frequency integral by

$$A_{132} = \frac{3\hbar'}{4\pi} \bar{\omega}_{132} \qquad (14)$$

for short-distance, "unretarded" interactions. Short-distance formulations are appropriate for this system, because nearly all the interaction energy is developed at very short separation distances compared to distances where retardation (62) becomes important.

Evaluation of Hamaker coefficients by Lifshitz theory will give information which can be used in the sphere-plate* Hamaker expressions (63)

$$U_{VdW} = -N_a \frac{A_{132}}{6} \left[\frac{2a_v(a_v + d_{ed})}{d_{ed}(d_{ed} + 2a_v)} - \ln \frac{(d_{ed} + 2a_v)}{d_{ed}} \right] \quad (15)$$

appropriate for our system to calculate Van der Waals potentials (U_{VdW}), selecting 0.1 nm for d_{ed}.

It is mathematically convenient to evaluate individual self-interaction coefficients, and evaluate complex coefficients by more recent developments.

We apply mixing laws derived by Bargeman and Van Voorst Vader (64)

$$A_{132} = \frac{3h}{16\pi^2 b_i} \frac{(A_{11}^{1/2} - A_{33}^{1/2})(A_{22}^{1/2} - A_{33}^{1/2})}{A_{33}^{1/2}(A_{11}^{1/2} - A_{22}^{1/2})} \ln \left[\frac{1 - \frac{16\pi^2 b_i}{3h} (A_{22}A_{33})^{1/2}}{1 - \frac{16\pi^2 b_i}{3h} (A_{11}A_{33})^{1/2}} \right] \quad (16)$$

and

$$A_{131} = \frac{(A_{11}^{1/2} - A_{33}^{1/2})^2}{1 - \frac{16\pi^2 b_i}{3h} (A_{11}A_{33})^{1/2}} \quad (17)$$

where b_i is a fitting parameter equal to $\sim 0.32 \times 10^{-16}$/s.

Self-interaction coefficients (A_{11}, A_{22}, A_{33}) are evaluated by Visser (65) from Lifshitz theory or Ninham and Parsegian's (66) macroscopic approximations. Appropriate values are presented in Table 8, along with mixed coefficients (A_{131} and A_{132}) calculated with equations 16 and 17.

To determine to what extent Van der Waals potentials account for the residual free energy controlling adsorption (ΔG_{res}), double layer contributions were subtracted from the overall free energy and the ΔG_{res} obtained was compared to U_{VdW} evaluated by Lifshitz-Hamaker theory. The comparison, presented in Table 9, shows that the Van der Waals potentials can account for all of the remaining energy. This means that the balance of double layer interaction and Van der Waals interaction can account for the principal contribution to virus adsorption free energies with these solids.

A value for d_{ed} (0.1 nm) was selected that is shorter than that used by other investigators, e.g. 0.2 nm (67) and 0.4 to 1 nm (65). This probably is in response to the larger contact area expected between virus and oxide surface than given by the sphere-plate interaction model, and also for possible effects of solution damping (61).

*Refer to Figure 5 for diagrammatic presentation.

TABLE 8. INDIVIDUAL SELF-INTERACTION HAMAKER COEFFICIENTS TAKEN FROM VISSER (65) AND CALCULATED MIXED COEFFICIENTS

Material	A_{11} Values - erg x 10^{-13}	Theory
Water	4.38	Lifshitz
Polystyrene (virus)	6.15-6.60	"
"Oxides, etc."	10.6-15.5	"
Metals	16.2-45.5	"
Quartz	8.0-8.8	Macroscopic Approximation
Material	**A_{132} Values - erg x 10^{-13}**	**Theory**
Quartz-Water-Virus	0.33-0.49	Bargeman and Van Voorst Vader
"Oxides"-Water-Virus	0.53-1.06	
"Metal"-Water-Virus	0.91-2.97	
Polystyrene-Water-Virus	0.17-0.26	

TABLE 9. COMPARISON OF LIFSHITZ-VAN DER WAALS POTENTIALS TO RESIDUAL FREE ENERGY COMPONENTS AFTER CORRECTING FOR DOUBLE LAYER REPULSION

Solid	U_{VdW} - kJ/mol	ΔG_{res} - kJ/mol
α-SiO_2	-43.0 to -63.9	-51.9 ± 3.2*
α-Fe_2O_3	-69.1 to -138	-61.0 ± 1.2
β-MnO_2	"	-66.1 ± 2.1
CuO	"	-73.7 ± 5.0
Al Metal	-118 to -387	Very Strong†
Polystyrene	-22.2 to -33.9	Weak - No Ads.

*Values are standard deviations.
†Irreversible reactions, ΔG_{ads} could not be determined.

Lifshitz theory predicts that we should have stronger adsorption on Si metal than on SiO_2. This effect is not observed in our adsorption results. It is suspected that kinetic difficulties in approach to the Si metal surface or the thickness of the oxide coating* on the metal may prevent strong adsorption.

On Al metal, however, even though ellipsometry† suggests an oxide coating we see exceptionally strong adsorption, characteristic of metal predictions by Lifshitz theory. This may involve local thin spots in the coating allowing dipole-dipole contributions from the metal proper to interact with adsorbing virus.

In any case, with the Lifshitz theory and also with double layer interaction theory, the conditions for accepting the models – viz. correspondence of potentials with free energies and reasonable values for characteristic separation distances, have been met.

OTHER POSSIBLE COMPONENTS

Even though DLVO-Lifshitz theory explains virus adsorption with surprising accuracy, it should be recognized by the critical investigator that the fit could be merely coincidental.

We are unable to develop models substantiating significant involvement of covalent-ionic interactions, hydrophobic interactions, and electrostatic induced image interactions being important in virus adsorption to materials studied here. This topic is discussed at length in (34) and (70). Minor contributions from ΔG_{ads} nonetheless, may come from these other types of interaction in some cases.

The estimate of ~50 interfacial water molecules displaced by adsorption of one virus particle suggests that energy not accounted for previously is required for this transfer. LeNeveu et al's. (71) measurements of the chemical potentials of hydration associated water molecules are 0.2 kJ/mol to 0.01 kJ/mol at 0.4 to 1.0 nm phospholipid bilayer separations. For the virus system this gives an estimated 0.5 to 10 kJ/mol repulsive energy due to transfer of hydration water to the bulk liquid. The precision to which DLVO-Lifshitz theory can be fit to free energy data could easily accommodate this level contribution to ΔG_{ads}.

Ion-exchange concepts are inapplicable to our problem because viruses are orders of magnitude larger than ions. Ion exchange occurs as a result of charge development on surfaces of materials (35). In our system, these developments are expressed in the interaction of double layers.

---

*3 to 6 nm thick by ellipsometry for Si exposed to air for several months (68).

†Smith (69) found by ellipsometry that the oxide coat on Al metal is ~5 nm thick after electropolishing in $HClO_4$-ethanol mixtures and ~20 nm thick after acid-dichromate etching.

Good fit of the DLVO-Lifshitz theory suggests that additional entropy contributions may be small.

PREDICTIONS FROM DLVO-LIFSHITZ THEORY

The DLVO-Lifshitz theory is capable of predicting adsorption characteristics of viruses in aquatic systems.

For spherical particles, keeping all other parameters constant, if Eq. 8 is combined with Eq. 15, and the combined double layer and Van der Waals potential is varied with particle radius, large particles are predicted to adsorb more strongly than small ones. In general, Wallis and Melnick's empirical studies (72) of the adsorption of various virus types on aluminum hydroxide and phosphate precipitates exhibit this trend, but there is considerable scatter in the correlation. Adenoviruses and reoviruses, which are larger than enteroviruses, adsorb less strongly than enteroviruses to these precipitates. Differences in electrokinetic properties and the configuration of the interaction with the surfaces due to different viral architectures are thought to be the cause of this apparent discrepancy.

Tailed bacteriophages are morphologically very different from enteroviruses. In these phages, in contrast to enteroviruses, different types of protein are found in different locations on the virion surfaces and their electrical properties are expected to be considerably different. Adsorption of these phages should be unrepresentative of enterovirus adsorption. Icosahedral phages such as f2 may correspond to enteroviruses in terms of the configuration of the interaction, but if their electrical properties are much different, adsorption characteristics may be different as well.

The combined DLVO-Lifshitz expression predicts that if the virus and solid have similar charge, increasing the ionic strength of the supporting solution will increase the tendency of virus to adsorb. Conversely, if they are of opposite charge, an increase in ionic strength will decrease the tendency to adsorb.

Using SiO_2 ζ measurements, and for Mandel's (70) poliovirus - estimating the zeta potentials by Hunter and Wright's correlation and the Nernst equation, Eq. 8 can be used to estimate the effect of pH on adsorption. The Van der Waals component -51.9 kJ/mol for SiO_2 was taken from Table 9. An ionic strength of 0.02 with monovalent cations and anions was selected. Our prediction is presented in Figure 6. The pH at which the isoelectric point shifts from the A to the B conformation was taken from Mandel's (56) data. It may, actually, shift when adsorbed to a surface at a different pH.

At high pH (8 to 9) the adsorbed fraction of total virus present in the system (F_{ads}) is very small. As the A state isoelectric point is approached about pH 7, adsorption is strong. It decreases on lowering the pH between 5 and 6, however, until transition to the B state occurs and we have strong adsorption again around pH 4.5. Of course, differences in electrical properties with different adsorbents will change predicted adsorption on these materials to be noticeably different from SiO_2. Some investigations such as those of Berg (4) who found an adsorption maximum at pH 7 on membrane filters

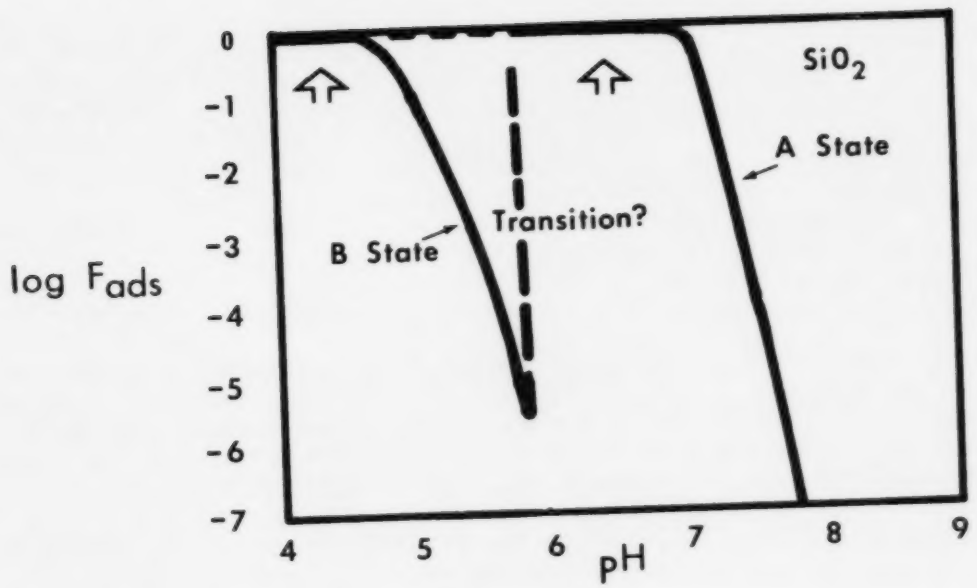

Figure 6. Estimated variation of poliovirus adsorption with pH on one m^2 of α-SiO_2 at 0.02 ionic strength as predicted by DLVO theory. Transition from the A to B state is taken from Mandel. Arrows represent pH regions of relatively strong predicted adsorption.

with poliovirus and those of Netty Buras (personal communication, 1976) who found adsorption maxima at about pH 7 and pH 4.5 on magnetite (Fe_3O_4) but decreased adsorption at intermediate pHs, agree with DLVO-Lifshitz predictions in Figure 6. Other studies such as those of Gerba et al. (73) on poliovirus adsorption to activated carbon, however, do not show the two maxima expected.

Lifshitz theory predicts that materials with high dielectric susceptibilities such as metals and metal sulfides, should develop higher Van der Waals potentials, and therefore be better virus adsorbents than materials such as silicate minerals, clay minerals, and humic substances, i.e.,

$$\underset{\text{(strong)}}{\text{Metals}} > \text{Sulfides} \geq \underset{\text{Oxides}}{\text{Transition Metal}} > SiO_2 \text{ etc.} > \underset{\text{(weak)}}{\text{Most Organics}}$$

The surface area of a given material must also be taken into account. Large amounts of surface area favor more adsorption. Care must be taken when extending this generalization to porous materials such as activated carbon and clay minerals, however, because the surface area included in pores may not be accessible to adsorbing virus. Additional discussion of environmental implications has been presented earlier (34, 70).

Aluminum metal appears to be particularly good in regard to adsorbing virus. This material will be examined in greater detail in following sections concerning virus degradation and removal in column experiments.

SECTION 6

DEGRADATION OF POLIOVIRUS BY ADSORPTION

KINETIC APPROACH

In the last section, the principal mechanisms by which virus particles adsorbed to various solids were resolved. Another critical question that deserved attention was whether or not virus retained or lost infectivity during or after adsorption. This question was investigated by study of the infectivity and labeled viral protein and nucleic acid concentrations recovered in desorption experiments.

Only on SiO_2 could all ^{3}H-RNA and ^{14}C-protein be recovered in one extraction. All other solids allowed only a small fraction of the radioactivity initially adsorbed to be eluted. Lack of recovery of virus from various adsorbents is a widely recognized phenomenon (74). The question of whether this lack of recovery represents strong adsorption or inactivation will now be addressed. Kinetic theory applied to infectivity and radioactivity data from multiple extractions provides an answer to this question. It allows calculation of total virus (both infectivity and radioactivity) recoverable with an infinite number of extractions. Comparisons between stock preparations and desorbed virus can then be made for estimates of specific infectivity loss.

Derivation of Kinetic Expressions

For multiple extraction data, the mass balance expression can be written

$$Ads_{n-1} - Ads_n = C'_n V_n \tag{18}$$

where Ads_n is the total virus adsorbed for extraction n, C'_n is the concentration due to desorption during step n, V_n is the volume, and n-1 refers to the previous extraction.*

A first-order rate of virus desorption from the surface

$$\frac{d\,Ads}{dt} = -k\,Ads \tag{19}$$

---

*Variables Ads, C' and others pertaining to amounts of virus can refer to either infectivity or radioactivity.

where k is the rate constant and t is elapsed time was applied because surface coverage (<<1%) is low, which minimizes the probability of particle-particle interactions. Other systems, that have high surface coverage, could have significant adsorbate-adsorbate interactions on the surface which could cause desorption reactions to have orders different from one. No back reaction occurs during elution because controls demonstrated that virus does not adsorb to any of our solids in the presence of our elution medium. We also assume that $dk/dn \rightarrow 0$ for our systems, and this assumption is evaluated during discussion of these results.

Substitution and integration of Equations 18 and 19 gives

$$V_n C'_n = Ads_{n-1}[1 - \exp(-k\Delta t)]. \tag{20}$$

Since

$$\frac{Ads_n}{Ads_{n-1}} = \exp(-k\Delta t) \tag{21}$$

for any n,

$$C' = D\,Ads \tag{22}$$

where

$$D = \frac{\exp(k\Delta t) - 1}{V}$$

and substituting into Eq. 18 we have

$$C'_n - C'_{n-1} = C'_n\, DV_n. \tag{23}$$

Keeping V and Δt invariant with respect to n, and assuming that our extractions are a continuous process, we have

$$\frac{dC'}{C'} = -DV\, dn \tag{24}$$

Integrating this expression gives

$$\ln C' \Big|_o^x = -DV\, n \Big|_o^x \tag{25}$$

where x represents the sequence number of the final extraction. Plotting ln C' versus n will give a straight line with slope -DV and intercept $\ln C'_o$.

The amount recoverable in an infinite number of extractions is then

$$Ads_o = \frac{C'_o}{D} \tag{26}$$

by Eq. 22.

DEGRADATION EXPERIMENTS

Degradation studies were performed on all solids used for the adsorption mechanism studies except Si metal. A different batch of SiO_2 with a slightly greater surface area (Table 1) was used in these experiments.

Experiments were done in ethylene oxide or UV sterilized polyethylene scintillation vials. Virus was adsorbed to the solids for periods of two hr to 24 hr in 10 ml of 0.02 I NaCl + $NaHCO_3$ pH 7 buffer at 15 ± 2°C prior to elution. The following weights of solids were used in the experiments; values after ± represent standard deviations:

α-SiO_2	4.02 ± 0.01 g (initial), 2.64 ± 0.06 g (residual, w_r)
α-Fe_2O_3, β-MnO_2, CuO, Al metal	1.00 ± 0.01 g
α-Al_2O_3	0.0803 ± 0.0002 g

Experiments with SiO_2

On SiO_2, after virus was adsorbed to the solids for the incubation time periods mentioned above, the mixture was sampled and 10x concentrated elution medium was added in the appropriate amount. The samples were then placed on the sample rotator and eluted at 25 ± 2°C for one hr for extraction. Afterwards, they were centrifuged in an IEC model PR-2 refrigerated centrifuge for 5 min at 250g and sampled.

Both aliquot sampled after adsorption and that sampled after elution required additional clarification at 15,000g for 10 min in a Spinco model L ultracentrifuge with a 40.2 rotor.

The liquid volumes were monitored at every step during the experiment by recording the pipetted input volumes or weighing. The amount of silica withdrawn from the reaction vessels was determined by rinsing the solid portion of the withdrawn aliquot after sampling with ddd H_2O and weighing after drying at 200°C.

The amount of virus initially adsorbed (Ads_i) is

$$Ads_i = \frac{w_r}{w_a} \quad (Tot - V_a C_u) \tag{27}$$

where

Tot = total virus initially added,

w_r = amount of solid remaining in reaction vessel after sampling,

w_a = total solid initially added,

V_a = solution volume in reaction vessel during adsorption,

C_u = concentration of virus not initially adsorbed.

The recovered virus (Ads_r) is

$$Ads_r = C_e V_e - C_u V_r \tag{28}$$

where C_e is the virus concentration after elution, V_e is the volume of eluting solution in the reaction vessel, and V_r is the residual volume of solution left after withdrawing the aliquot to determine unadsorbed virus.

Experiments with Other Solids

To obtain degradation information on other solids it was necessary to perform multiple extractions and apply the kinetic analysis derived earlier.

Virus was adsorbed to solids under the same conditions used for SiO_2 for periods of two hr and 24 hr.

The samples were then centrifuged for 5 min at 250g in the PR-2 refrigerated centrifuge and sampled for residual virus. The supernatants were then aspirated and 10 ml of elution medium (1x) were added to the reaction vessels. The samples were placed on the rotator and eluted for 15 min at 25 ± 2°C followed by 5 min centrifugation at 250g in the PR-2, sampling for eluted virus, and aspiration of the remaining medium. This procedure was repeated four times in sequence. All volumes were monitored during the experiment by pipetting or weighing.

The total virus initially adsorbed is

$$Ads_i = Tot - V_a C_u. \tag{29}$$

For calculation of the amount of material recoverable with an infinite number of extractions (Ads_o), concentrations in the elution supernatants which desorb during the given extraction (C'_n...) are required. They are obtained from analyzed concentrations (C_n) by

$$C'_n = C_n - C_{n-1}\left(\frac{V_r}{V_n}\right) \tag{30}$$

where V_r is the volume of residual buffer or elution medium left in the reaction vessel from the previous operation.

The value of Ads_o can then be obtained from the expression derived earlier,

$$Ads_o = \frac{C'_o}{D} \qquad (26)$$

where values of C_o and D are obtained by linear regression analysis of C' data.

Controls for these experiments showed that there was no significant loss of virus or infectivity in the reaction vessels when incubated with 0.02 I buffers pre-equilbrated ($\geq$ 1 week) with solid phases. Elution media had no significant effect on the virus titer for times equal to those used for extraction experiments, and no significant effect on the HeLa cell assay system when diluted 1:30 or greater with media used to prepare serial dilutions. Theoretical minimum estimates of standard deviations of initially added virus and recovered virus were made from analysis of data scatter about regression lines and theoretical counting plus pipetting variations. Other sources of variation, such as differences in site-specific interaction energy over the surface, cannot be quantified at present. Duplicate determinations indicate slightly greater variation than theoretically predicted.

RESULTS

If all infectivity, ^{3}H-RNA, and ^{14}C-protein initially adsorbed within expected variation of the system is recovered, virus is not significantly inactivated by the presence of the surface. If all ^{3}H-RNA and ^{14}C-protein is recovered but significant losses of infectivity are observed, we can conclude that virus is inactivated and not just merely adsorbed. These hypotheses are valid even if preparations contain minor levels of radioactive impurities, provided that we have no additional inactivation due to the combined effects of adsorbent and elution medium.

Recovery information for SiO_2 is presented in Table 10. All the infectivity, ^{3}H-RNA, and ^{14}C-protein initially adsorbed is recovered and no significant loss of infectivity is observed for the two hr and 24 hr samples.

For other solids, application of the kinetic theory derived earlier is required to determine whether or not virus is being inactivated by adsorption on the surface. The kinetic plot mentioned earlier gives us additional information concerning degradation. If regression lines of normalized (C'/Ads_i) concentration data are coincident, virus infectivity is not altered, provided that degradation products desorb in the elution medium. If regression lines are linear, the assumption regarding the invariance of desorption rate with extraction sequence number is indicated to be appropriate. Recovery information is presented in Tables 11 to 15 and sample kinetic plots (sample C for all cases) are presented in Figures 7 to 11.

TABLE 10. COMPARISON OF VIRUS INITIALLY ADSORBED (Ads_i) WITH VIRUS RECOVERED (Ads_r) for α-SiO_2

Measurement	Sample	Ads_i	Ads_r
2-hr Incubation — Duplicates A,B			
Infectivity (log PFU)	A	8.46 ± 0.08*	8.71 ± 0.10
	B	8.41 ± 0.09	8.63 ± 0.11
^{3}H-RNA (log CPM)	A	3.22 ± 0.02	3.17 ± 0.03
	B	3.17 ± 0.03	3.12 ± 0.04
^{14}C-Protein (log CPM)	A	3.20 ± 0.02	3.13 ± 0.03
	B	3.15 ± 0.03	3.13 ± 0.03
24-hr Incubation — Duplicates C,D			
Infectivity (log PFU)	C	8.46 ± 0.10	8.14 ± 0.10
	D	8.49 ± 0.10	8.30 ± 0.09
^{3}H-RNA (log CPM)	C	3.41 ± 0.03	3.38 ± 0.04
	D	3.49 ± 0.02	3.56 ± 0.03
^{14}C-Protein (log CPM)	C	2.29 ± 0.02	2.86 ± 0.03
	D	2.99 ± 0.02	2.96 ± 0.03

PFU = plaque forming units, CPM = counts per minute.

*Values are standard deviation estimates.

On Fe_2O_3 as with Al_2O_3 there is a possibility that inactivation of virus occurs on the surface, but it does not appear very significant. On MnO_2 we see demonstrable amounts of inactivation, both by examining recovery information and by observing that the regression lines of normalized infectivity data plot distinctly below radioactivity data. On CuO, inactivation is quite marked by the criteria mentioned above. In addition, the amount of virus inactivated increases with the length of time virus was incubated with the adsorbents prior to extraction.

On aluminum metal, however, inactivation is quite dramatic. For two-hr samples, recovered infectivity is decreased approximately three orders of magnitude compared to that initially adsorbed. For 24-hr samples, greater than four orders of magnitude decrease was observed. Only with the first extraction was any infectivity (86 PFU/ml) detectable. A minimum value for

TABLE 11. COMPARISON OF VIRUS INITIALLY ADSORBED (Ads_i) on α-Fe_2O_3 WITH VIRUS RECOVERED BY KINETIC ANALYSIS OF DATA FROM FOUR EXTRACTIONS (Ads_o)

Measurement	Sample	Ads_i	Ads_o
2-hr Incubation — Duplicates A,B			
Infectivity (log PFU)	A	8.61 ± 0.06*	8.33 ± 0.20
	B	8.61 ± 0.06	7.56 ± 0.10
^{3}H-RNA (log CPM)	A	3.58 ± 0.02	3.20 ± 0.21
	B	3.58 ± 0.02	3.19 ± 0.23
^{14}C-Protein (log CPM)	A	3.41 ± 0.02	3.31 ± 0.31
	B	3.41 ± 0.02	3.27 ± 0.34
24-hr Incubation — Duplicates C,D			
Infectivity (log PFU)	C	8.14 ± 0.07	7.74 ± 0.25
	D	8.14 ± 0.07	7.75 ± 0.32
^{3}H-RNA (log CPM)	C	3.74 ± 0.02	3.53 ± 0.16
	D	3.74 ± 0.02	3.50 ± 0.11
^{14}C-Protein (log CPM)	C	3.18 ± 0.02	3.02 ± 0.21
	D	3.19 ± 0.02	2.87 ± 0.08

PFU = plaque forming units, CPM = counts per minute.

*Values are standard deviation estimates.

the slope of -0.2 was estimated here, less than half that found with the two-hr samples. This gives a conservative estimate for recovery of infectivity. The less than 10^4 PFU detection limit is imposed by the requirement of diluting elution medium 1:30 or more for assay, and by constraints defined by the mathematics of the system. A lower bound on the amount inactivated can be predicted from PFU assays and extraction volumes. Both duplicates contained 1 PFU per inoculated extraction media volume. This gives approximately 10^3 PFU recovered for the total volumes used during the first extractions of the aluminum metal recovery experiment.

The logarithms of extraction concentration data approach linearity when plotted as a function of n, but exhibit a slightly concave upwards trend in some cases. This indicates that materials desorb from a given surface with similar but not quite identical rates.

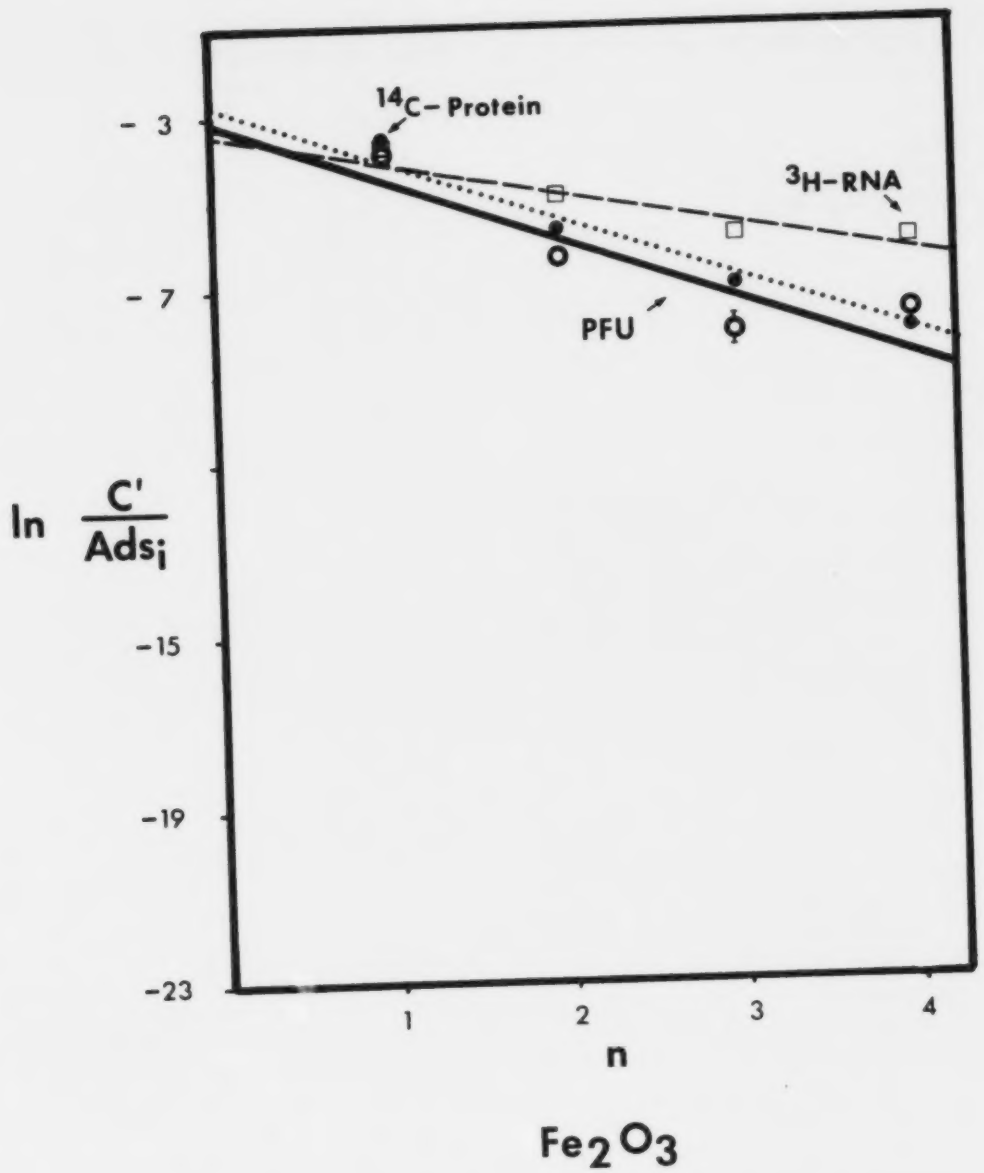

Figure 7. Kinetic plot for α-Fe_2O_3, Sample C. C'/Ads_i is the concentration of virus that desorbs during each sequential extraction, n = 1 to 4; divided by the total virus initially adsorbed to the solid. Plotted curves are least square fit linear regressions. The error bar represents theoretical assay standard deviation.

TABLE 12. COMPARISON OF VIRUS INITIALLY ADSORBED (Ads_i) on β-MnO_2 WITH VIRUS RECOVERED BY KINETIC ANALYSIS OF DATA FROM FOUR EXTRACTIONS (Ads_o)

Measurement	2-hr Incubation — Duplicates Sample	Ads_i	Ads_o
Infectivity (log PFU)	A	8.57 ± 0.09*	7.53 ± 0.36
	B	8.57 ± 0.09	7.86 ± 0.11
^{3}H-RNA (log CPM)	A	2.93 ± 0.02	3.09 ± 0.15
	B	2.93 ± 0.02	3.09 ± 0.20
^{14}C-Protein (log CPM)	A	3.14 ± 0.02	3.05 ± 0.09
	B	3.14 ± 0.02	2.97 ± 0.19
Measurement	24-hr Incubation — Duplicates Sample	Ads_i	Ads_o
Infectivity (log PFU)	C	8.37 ± 0.13	7.13 ± 0.24
	D	8.37 ± 0.13	7.43 ± 0.31
^{3}H-RNA (log CPM)	C	3.73 ± 0.02	3.04 ± 0.24
	D	3.74 ± 0.02	3.02 ± 0.23
^{14}C-Protein (log CPM)	C	3.15 ± 0.02	2.70 ± 0.19
	D	3.16 ± 0.02	2.68 ± 0.18

PFU = Plaque forming units, CPM = counts per minute.

*Values are standard deviation estimates.

This is also seen in the slight decrease in recovery of ^{3}H-RNA and ^{14}C-protein seen in some samples. The decrease is barely measurable if at all, however, which suggests that the invariant rate constant assumption used here introduces little error in the recovery calculation.

DEGRADATION BY ALUMINUM METAL

In some cases, especially CuO, ^{3}H-RNA data points and regression lines are widely separated from ^{14}C-protein information. This indicates that ^{3}H-RNA and ^{14}C-protein are desorbing differently and suggests that the virus is being degraded by the surface.

To investigate this problem further, the experiment with Al metal where inactivation is most pronounced was repeated, but this time extracting once into a small volume using 10x elution medium as described for SiO_2. The eluted material was then layered on top of 15 to 30% RNAse-free sucrose gradients prepared in 0.02 I buffer at pH 8.4, equilibrated with atmospheric CO_2. Gradients containing virus from a parallel control which did not contain

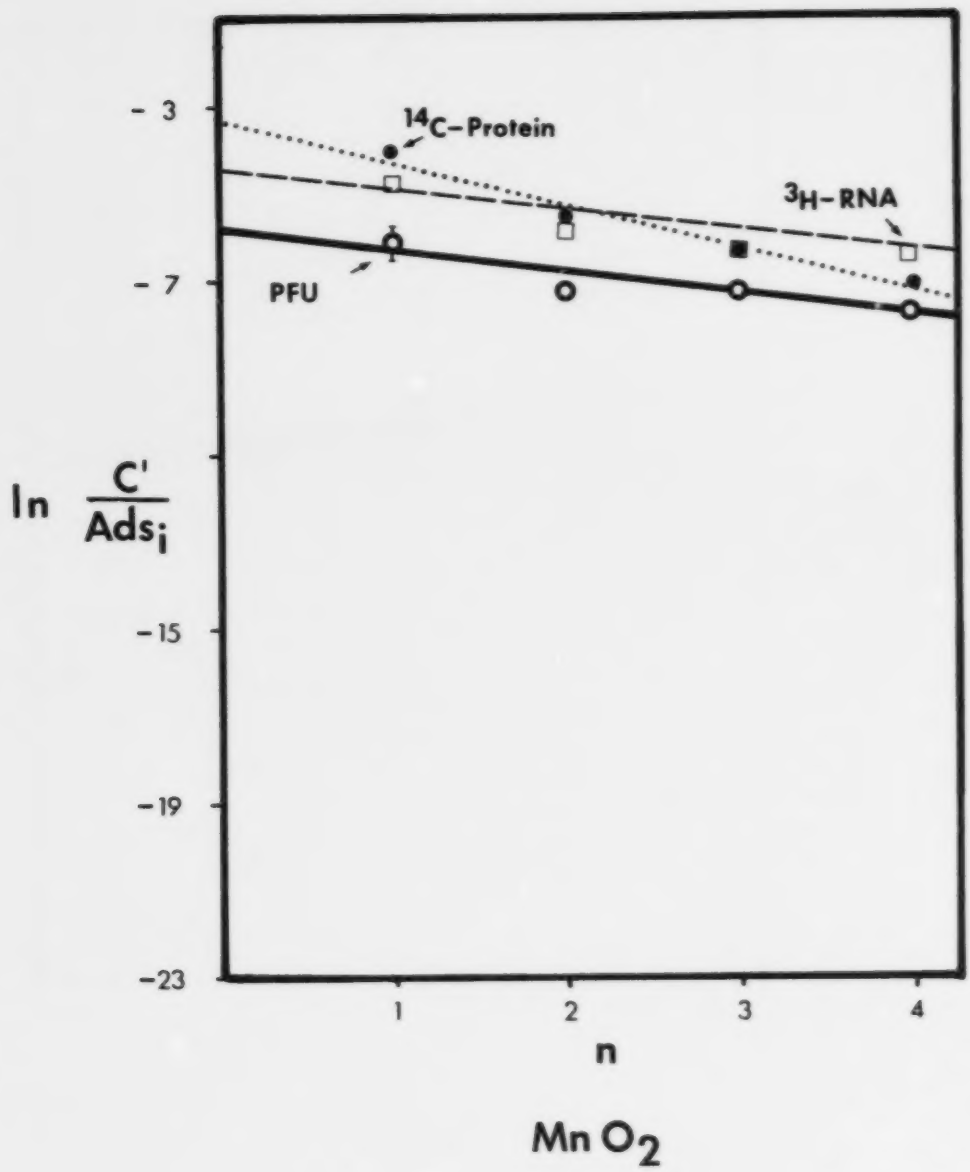

Figure 8. Kinetic plot for β-MnO_2, Sample C. C'/Ads_i is the concentration of virus that desorbs during each sequential extraction, n = 1 to 4; divided by the total virus initially adsorbed to the solid. Plotted curves are least-square fit linear regressions. The error bar represents theoretical assay standard deviation.

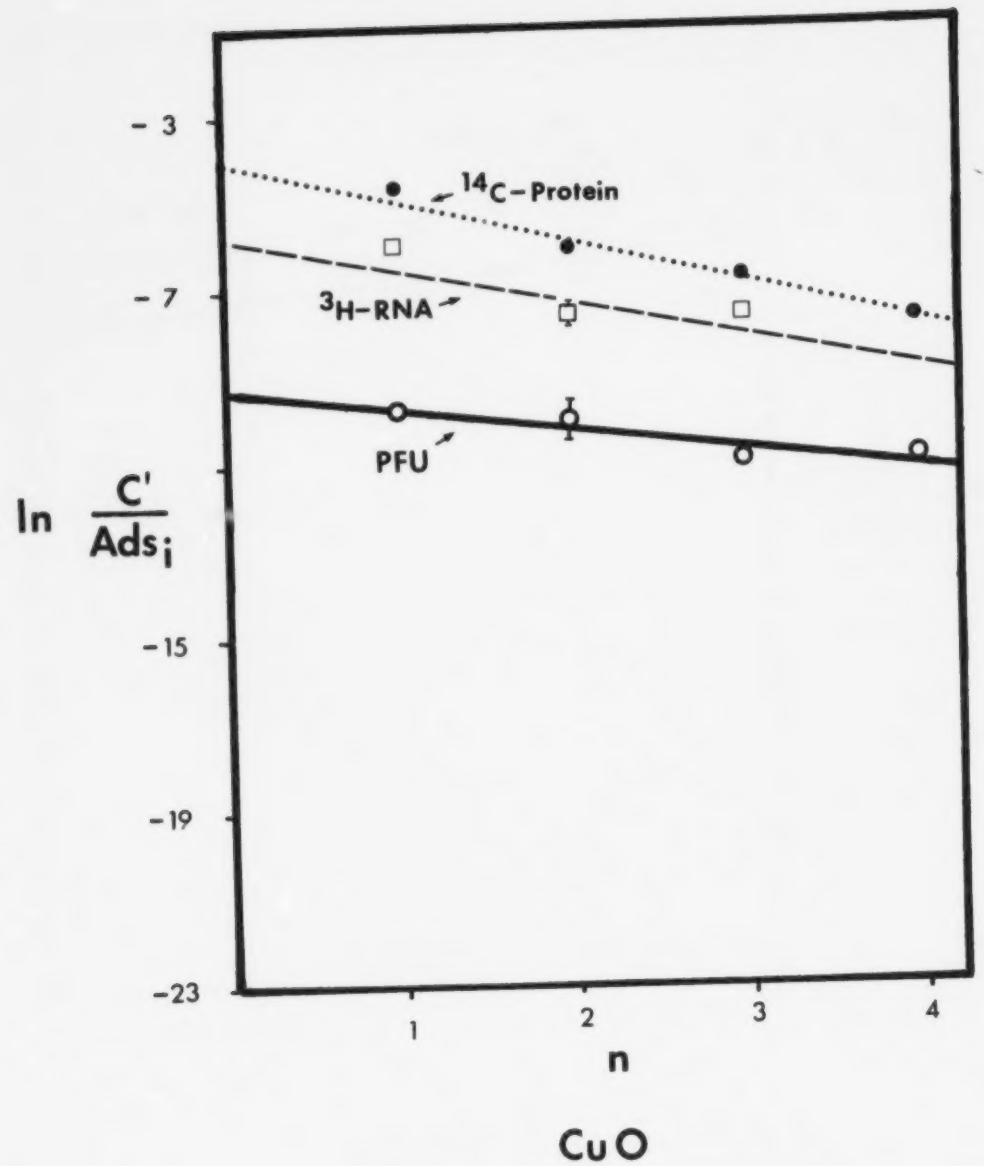

Figure 9. Kinetic plot for CuO, Sample C. C'/Ads_i is the concentration of virus that desorbs during each sequential extraction, n = 1 to 4, divided by the total virus initially adsorbed to the solid. Plotted curves are least-square fit linear regressions. The error bar represents theoretical assay standard deviation.

TABLE 13. COMPARISON OF VIRUS INITIALLY ADSORBED (Ads_i) on CuO WITH VIRUS RECOVERED BY KINETIC ANALYSIS OF DATA FROM FOUR EXTRACTIONS (Ads_o)

Measurement	Sample	Ads_i	Ads_o
2-hr Incubation — Duplicates A,B			
Infectivity (log PFU)	A	8.48 ± 0.09*	7.52 ± 0.32
	B	8.48 ± 0.09	6.76 ± 0.28
^{3}H-RNA (log CPM)	A	2.91 ± 0.02	1.97 ± 0.31
	B	2.92 ± 0.02	1.97 ± 0.43
^{14}C-Protein (log CPM)	A	3.09 ± 0.02	2.70 ± 0.13
	B	3.09 ± 0.02	2.60 ± 0.18
24-hr Incubation — Duplicates C,D			
Infectivity (log PFU)	C	8.65 ± 0.08	6.24 ± 0.17
	D	8.65 ± 0.08	6.51 ± 0.18
^{3}H-RNA (log CPM)	C	2.91 ± 0.02	1.62 ± 0.39
	D	2.92 ± 0.02	1.76 ± 0.22
^{14}C-Protein (log CPM)	C	3.11 ± 0.02	2.40 ± 0.16
	D	3.12 ± 0.02	2.40 ± 0.23

PFU = plaque forming units, CPM = counts per minute.

* Values are standard deviation estimates.

aluminum metal, and material eluted from Al metal surfaces were centrifuged in the Spinco model L ultracentrifuge for conditions presented in Figure 12. Fractions were collected for ^{3}H-RNA and ^{14}C-protein analysis.

Virus from the stock suspension sedimented at the expected 155S. A small amount of ^{3}H-RNA in the control separated from the virus and sedimented at 29S. Counts indicated in Figure 12 were normalized to represent the total counts in the elution medium for both the control and Al-eluted material.

Sedimentation coefficients were calculated using McEwen's (75) method and a virus density of 1.34 g/cm^3 (CsCl gradient) and RNA density of 1.66 g/cm^3 (76). Infectious RNA is reported to sediment at 32S to 35S (77).

TABLE 14. COMPARISON OF VIRUS INITIALLY ADSORBED (Ads_i) on α-Al_2O_3 WITH VIRUS RECOVERED BY KINETIC ANALYSIS OF DATA FROM FOUR EXTRACTIONS (Ads_o)

Measurement	Sample	Ads_i	Ads_o
2-hr Incubation — Duplicates A,B			
Infectivity (log PFU)	A	8.60 ± 0.07*	9.22 ± 0.41
	B	8.60 ± 0.07	8.60 ± 0.43
^{3}H-RNA (log CPM)	A	3.49 ± 0.02	3.43 ± 0.41
	B	3.49 ± 0.02	3.46 ± 0.38
^{14}C-Protein (log CPM)	A	3.39 ± 0.02	3.46 ± 0.33
	B	3.39 ± 0.02	3.54 ± 0.36
24-hr Incubation — Duplicates C,D			
Infectivity (log PFU)	C	8.73 ± 0.07	8.52 ± 0.85
	D	8.73 ± 0.07	7.86 ± 0.09
^{3}H-RNA (log CPM)	C	3.51 ± 0.02	3.24 ± 0.28
	D	3.51 ± 0.02	3.24 ± 0.31
^{14}C-Protein (log CPM)	C	3.46 ± 0.02	3.28 ± 0.28
	D	3.46 ± 0.02	3.26 ± 0.33

PFU = plaque forming units, CPM = counts per minute.

*Values are standard deviation estimates.

Virus eluted from aluminum metal was degraded into small fragments that remained at the top of the gradient. The degraded material at the top of this gradient contains far more labeled material than low molecular weight impurities present in the original preparation as seen in the control. This rules out the possibility that the material representing degraded virus could be due only to impurities in the original preparation.

DISCUSSION

Virus is degraded on aluminum metal and apparently not at all on Al_2O_3. Lifshitz calculations suggest that the metal should generate substantially stronger Van der Waals forces than the oxide. Earlier, it was suggested that partial penetration of the oxide coating known to be present on the

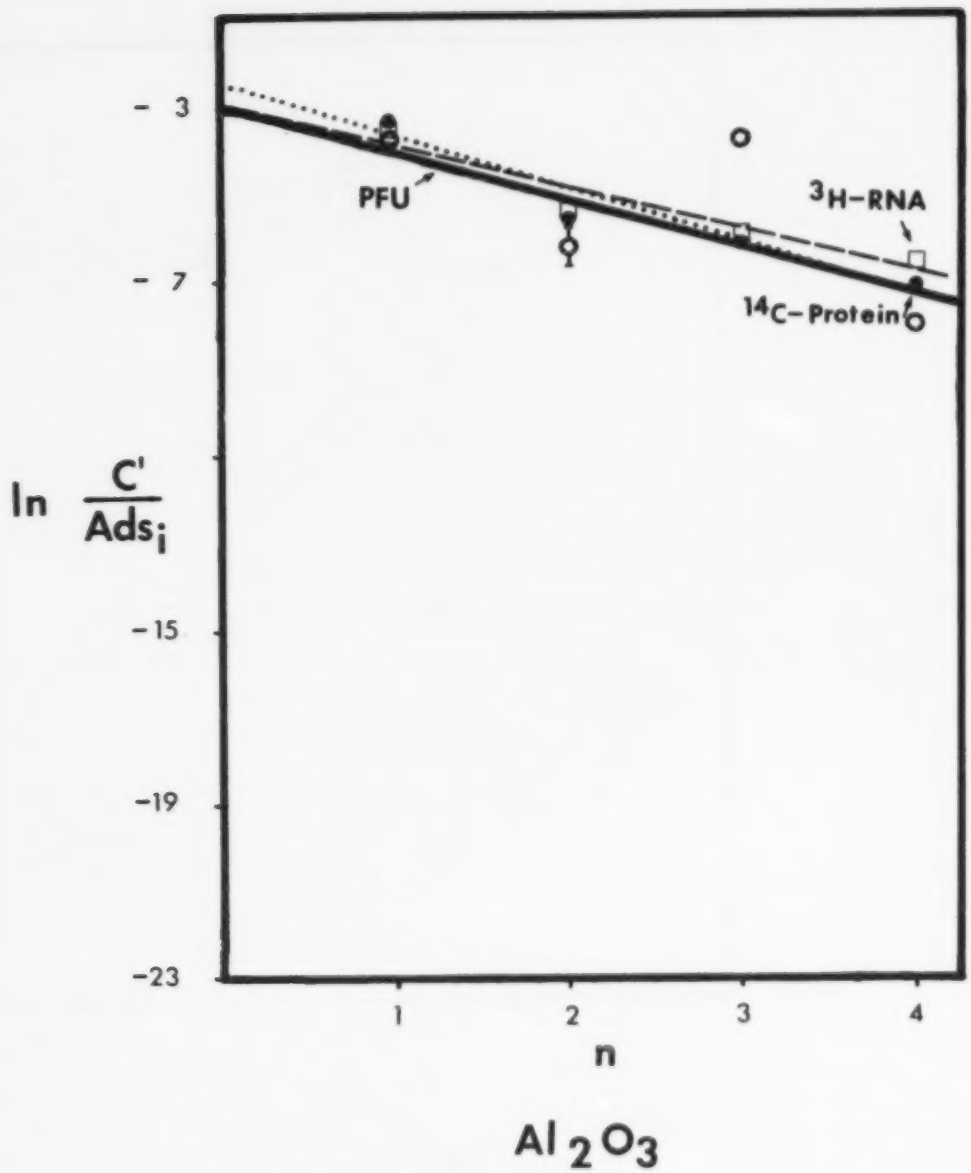

Figure 10. Kinetic plot for α-Al_2O_3, Sample C. C'/Ads_i is the concentration of virus that desorbs during each sequential extraction, n = 1 to 4, divided by the total virus initially adsorbed to the solid. Plotted curves are least-square fit linear regressions. The error bar represents theoretical assay standard deviation.

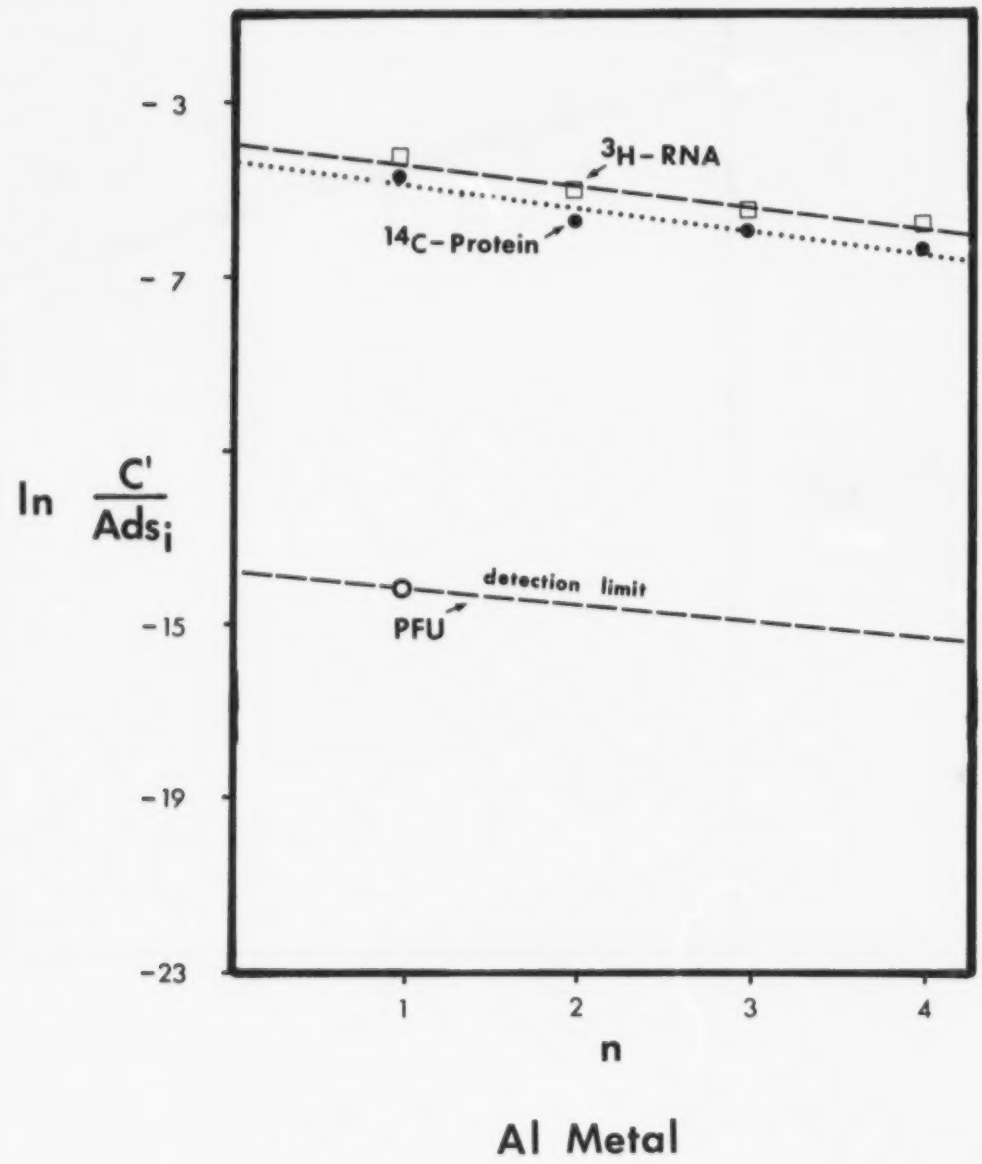

Figure 11. Kinetic plot for Al metal, Sample C. C'/Ads_i is the concentration of virus that desorbs during each sequential extraction, n = 1 to 4, divided by the total virus initially adsorbed to the solid. Plotted lines are least-square fit linear regressions.

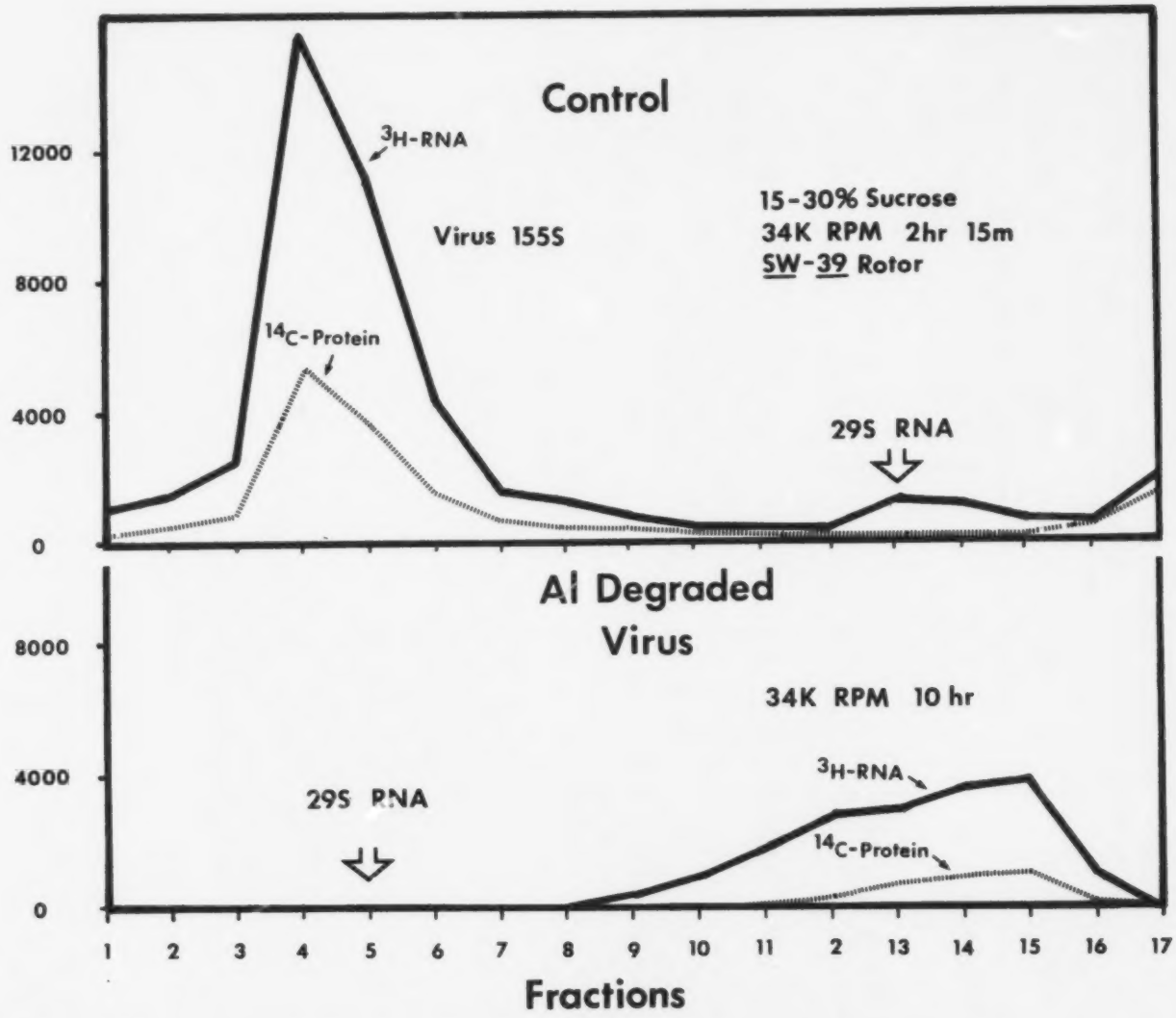

Figure 12. Sedimentation profiles of virus degraded by aluminum metal.

TABLE 15. COMPARISON OF VIRUS INITIALLY ADSORBED (Ads_i) on Al METAL WITH VIRUS RECOVERED BY KINETIC ANALYSIS OF DATA FROM FOUR EXTRACTIONS (Ads_o)

Measurement	Sample	Ads_i	Ads_o
2-hr Incubation — Duplicates A,B			
Infectivity (log PFU)	A	8.59 ± 0.07*	5.81 ± 0.46
	B	8.59 ± 0.07	5.96 ± 0.84
^{3}H-RNA (log CPM)	A	3.50 ± 0.02	3.40 ± 0.18
	B	3.50 ± 0.02	3.34 ± 0.19
^{14}C-Protein (log CPM)	A	3.44 ± 0.02	3.43 ± 0.14
	B	3.44 ± 0.02	3.38 ± 0.16
24-hr Incubation — Duplicates C,D			
Infectivity (log PFU)	C	8.27 ± 0.11	< 4
	D	8.27 ± 0.11	< 4
^{3}H-RNA (log CPM)	C	3.12 ± 0.05	2.73 ± 0.10
	D	3.11 ± 0.05	2.81 ± 0.05
^{14}C-Protein (log CPM)	C	3.32 ± 0.02	2.76 ± 0.09
	D	3.31 ± 0.02	2.69 ± 0.13

PFU = plaque forming units, CPM = counts per minute.

*Values are standard deviation estimates.

surface by these forces generated in the metal was responsible for the strong adsorbent properties of aluminum. These strong Van der Waals forces are suspected also to be involved in degradation, perhaps by stressing the adsorbed virion irreversibly.

The metal is demonstrated to be an effective substance for virus adsorption as well as degradation. This indicates that effective filters could be designed with aluminum metal to remove virus from aerosols and contaminated water and wastewater, if all pathogenic viruses react similarly.

Additional work must be done with viruses such as influenza, to confirm suspected broad-spectrum application to virus aerosol filters, and if possible, with hepatitis A for water and wastewater filters. In the next section, experimental application to water and wastewater systems will be presented.

SECTION 7

APPLICATION OF ALUMINUM METAL TO WASTEWATER DECONTAMINATION

INTRODUCTION

The final objective of the project is to determine whether or not materials selected by the first two studies could be effectively applied to decontamination of wastewater containing enteric viruses.

Studies of adsorption and degradation suggest that aluminum metal may be effectively applied to decontamination processes. In adsorption-filtration operations, we predict that it should be far better for virus removal than diatomaceous earth (78) or activated carbon (73). In addition, it is inexpensive and its very low levels of dissolution products, Al^{3+} and associated hydroxo complexes (35), are ubiquitous in natural waters and are considered non-toxic.

A potential problem with its application, however, may arise if organics present in water or wastewater block virus adsorption.

BENCH-SCALE PROCESS EXPERIMENT

A bench-scale process experiment was constructed to determine whether or not this blockage would occur with wastewater. The experiment was designed to be very conducive to rapid virus breakthrough, using a 1-cm thick bed of coarse aluminum metal powder and a residence time of only 0.7 min. With this design, if effective virus removals are obtained, there is good evidence that the material could be applicable to treatment plant conditions.

The apparatus is shown in Figures 13 and 14. Buffer (0.02 I - pH 7) was continuously pumped at 3.00 ± 0.01 ml/min with a Sage model 220 syringe pump into a magnetically operated flash mixing device at 15 ± 2°C. Shortly after the start of the experiment, ^{14}C-protein labeled virus suspended in 0.02 I buffer containing 1% fetal bovine serum to prevent loss of virus to the syringe needle, plus 1.32 (± 0.05) x 10^5 CPM/ml tritiated water (^3H-H_2O), was injected into the flash mixer. A Sage model 355 syringe pump was used with a flow rate of 3.29(± 0.07) x 10^{-3} ml/min for this injection. The input virus concentration was 1.14 (± 0.18) x 10^6 PFU/ml.

Midway during the experiment (~3hr), the reservoir delivering 0.02 I buffer was changed to one containing secondary effluent obtained from the Palo Alto treatment plant (Table 16) with an added 148 ± 6 CPM/ml ^3H-H_2O.* The

*The effluent was allowed to settle for 2 days at 4°C prior to this experiment to remove coarse suspended material which might stop flow in the tubing used with the syringe pumps. Total coliforms = 5.90 (± 0.87) x 10^4 per 100 ml.

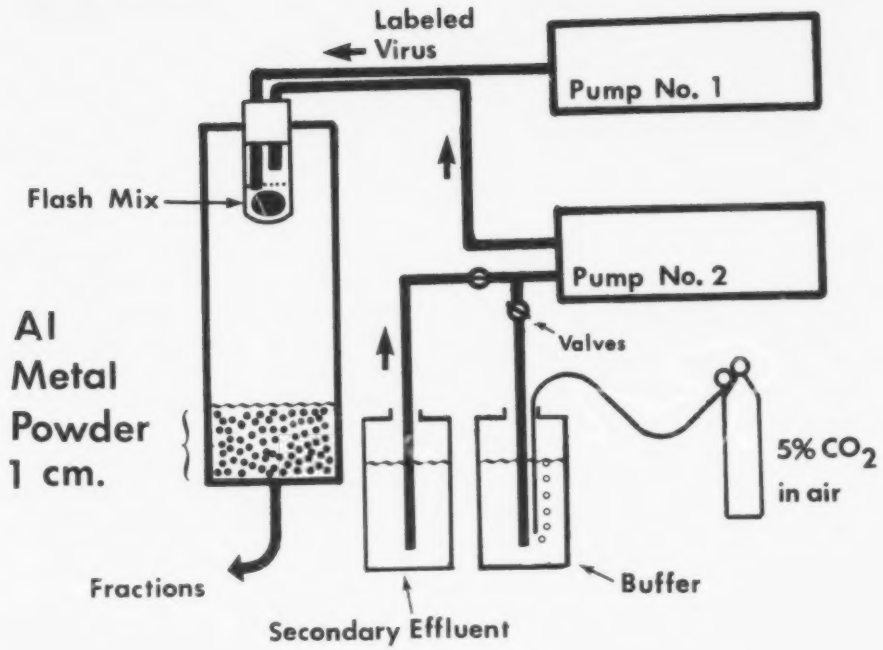

Figure 13. Schematic diagram of bench-scale process experiment.

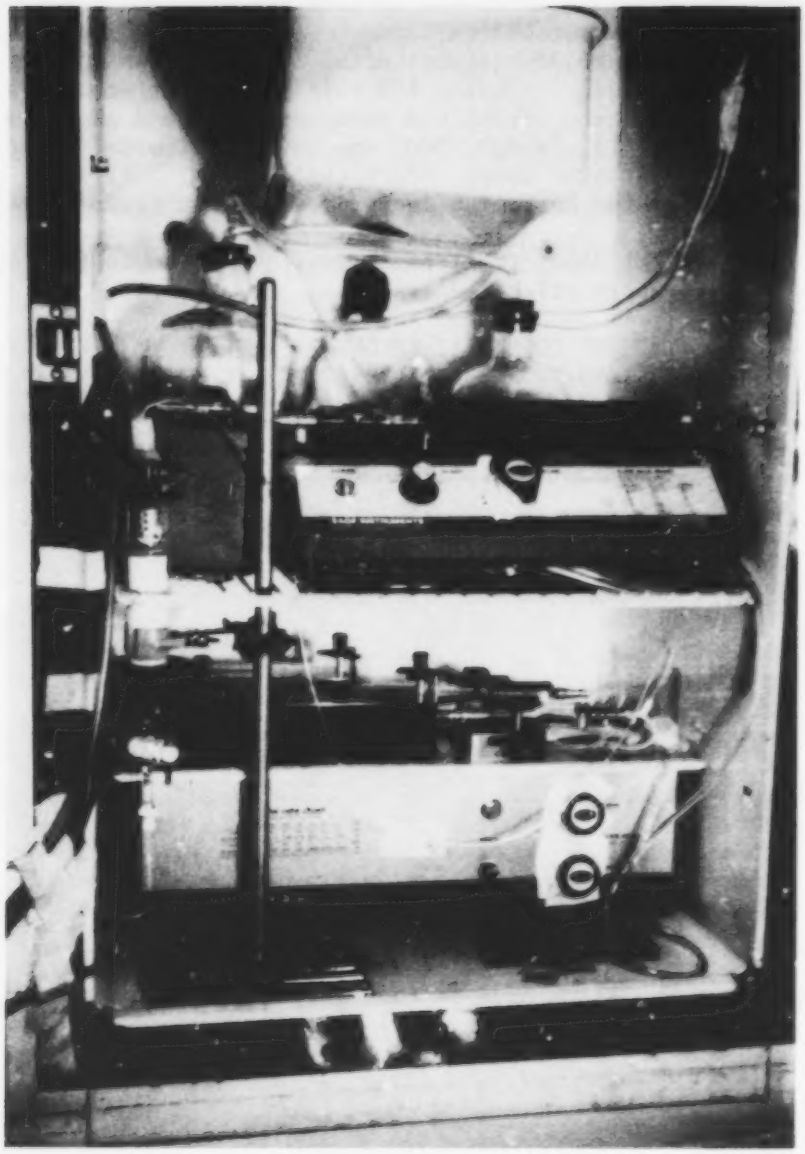

Figure 14. Photograph of Bench-Scale Process Experiment.

$^{3}H\text{-}H_2O$ in both the virus preparation and the effluent was included so the breakthrough of water associated with these solutions could be precisely determined, and any possible variation in flow rates would be detected.

The output of the column was collected into fractions until a total of 564 void volumes of fluid including 308 void volumes of secondary effluent had passed through the filter. Fractions were collected and analyzed for virus infectivity, ^{14}C-protein, $^{3}H\text{-}H_2O$, COD, and total coliforms. After sampling for the constituents listed above, fractions containing filtered secondary effluent were pooled for determination of residual suspended solids.

Comparison of the input (C_{in}) and output (C_{out}) concentrations is used to evaluate the filter's effectiveness.

TABLE 16. COMPOSITION OF COMPOSITE SECONDARY EFFLUENT (UNCHLORINATED) OBTAINED FROM PALO ALTO SEWAGE TREATMENT PLANT*

Constituent	Concentration (mg/l)
Total Solids	1000
Suspended Solids	30
Total Volatile Solids	15.1
Settleable Solids	5
BOD	30
COD	75
TOC	40
Chloride	305
NH_3-N	29.1
NO_3-N	<0.2
NO_2-N	0.05
Organic-N	5.25
Total Phosphorus	5.35
Turbidity	15 NTU
pH	7.6

*Data supplied by Mr. Ralph Nice of the Palo Alto sewage treatment plant.

RESULTS

Results of the experiment, presented as log C_{out}/C_{in} versus void volumes eluted, are presented in Figure 15. Breakthrough of virus infectivity occurs at ~130 void volumes. The steady-state concentration following breakthrough is 3.3 ± 0.6 orders of magnitude below the input concentration. Secondary effluent has no effect on the steady-state infectivity of the column output as compared to 0.02 I buffer. The large variation in the output infectivity is thought to be a result of the statistics of collision of virus with aluminum surfaces. C_{in} for $^{3}H\text{-}H_2O$ is taken to be the sum of the contributions from the virus stock and effluent. Output concentrations of $^{3}H\text{-}H_2O$ show

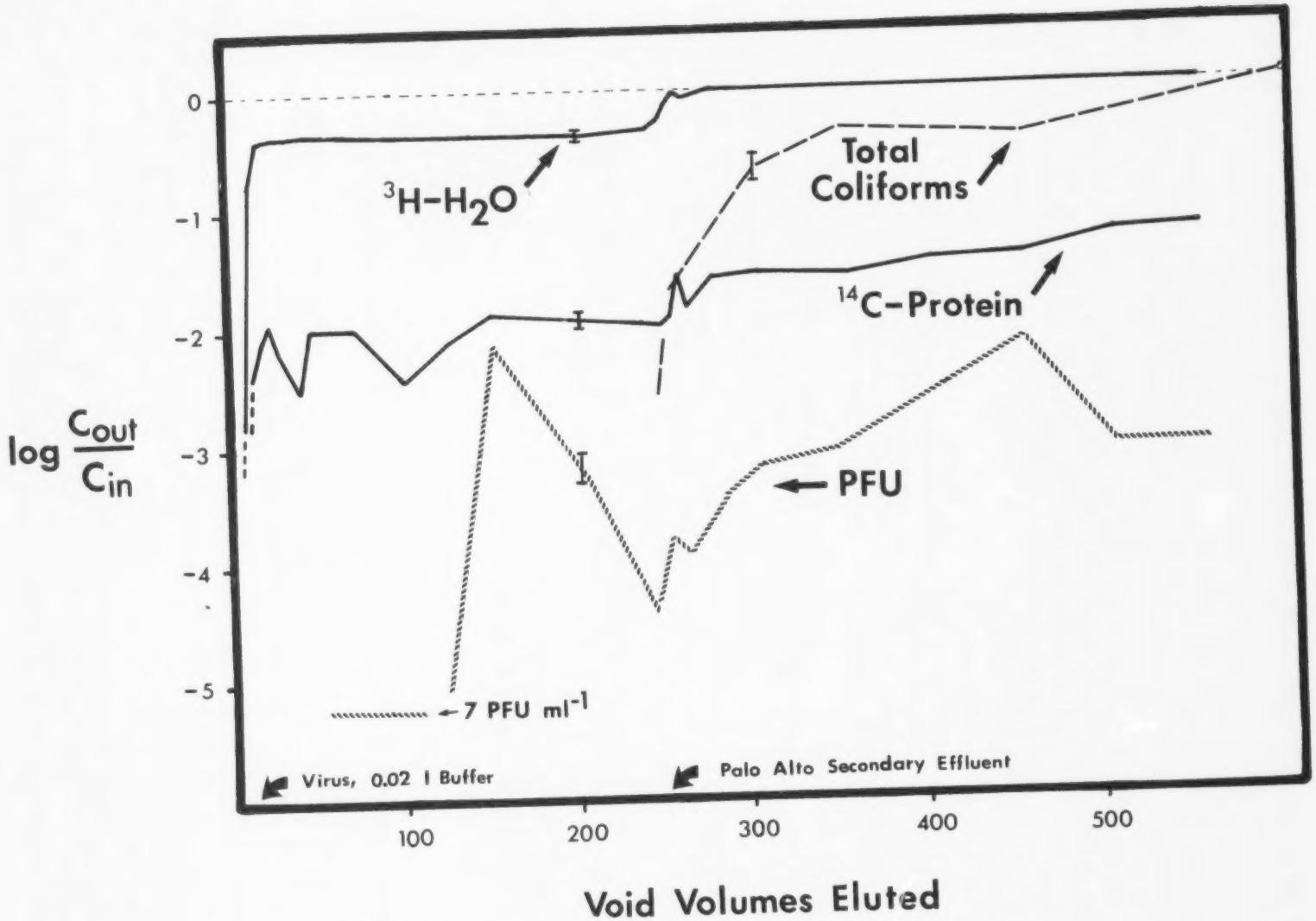

Figure 15. Results from Bench-Scale Process Experiment.

that fluid flow from the virus and buffer reservoirs remains constant during the experiment.

We find greater relative amounts of ^{14}C-protein in the column effluent than infectious virus. This represents a decreased tendency of virus degradation products or ^{14}C-labeled impurities to adsorb compared to infectious virus.

Coliform breakthrough begins at the same time as ^{3}H-H_2O breakthrough. ^{3}H-H_2O breakthrough indicates that secondary effluent replaced 0.02 I buffer in the column. A steady-state output coliform concentration reached that of the input, indicating that the bacteria are resistant to aluminum metal adsorption and degradation.

The concentrations of infectious virus, total coliforms, and other constituents in the input were determined by sampling the stock input fluids. Infectivity of the virus preparation was shown to be stable for at least 24 hr in Al equilibrated 0.02 I buffer. Incubation of virus with our secondary effluent for ~6 hr showed no significant loss in titer.

Total coliforms were determined immediately after sampling collected fractions. Since the stock and samples were assayed at the same time, the respective titers can be compared for recovery. If the coliform numbers in the stock effluent decreased in viability in the effluent during the course of the experiment, a similar decrease in viability in the collected fractions would be expected, because the solution conditions after filtration were essentially the same as in the stock.

The suspended solids concentration in input effluent was 1.0 mg/l and < 0.4 mg/l in pooled fractions. COD concentrations are listed below:

Input	Secondary Effluent (plus 1:1000 virus stock)		76 mg/l
	316-321	Void Volumes Eluted	78 mg/l
Output	418-423	" " "	54 mg/l
	546-551	" " "	52 mg/l

Only minor amounts of COD appear to be removed by the Al metal column.

Similar experiments with freshly precipitated manganese oxyhydroxides in the upper region of a 10 cm column of coarse SiO_2 did not give effective virus removals even with 0.02 I buffer conditions.

DISCUSSION

In Figure 15 we show that the virus infectivity in the Al metal output was dramatically reduced, and that secondary effluent did not inhibit adsorption, even after 300 void volumes had been eluted. The column was only 1 cm thick and the column had a residence time of only 0.7 min. If this degree of removal is extrapolated to a similar column 4 cm thick, made of the same aluminum powder - with identical flow rates, approximately 12 orders of magnitude reduction in virus titer is estimated by a first order removal rate.

Gerba *et al*. (73) studied poliovirus removal from filtered secondary effluent in 46 cm, 20 to 50 mesh, granular activated carbon columns with 3 min residence times. Breakthrough of PFU occurred at ~10 bed volumes and the steady-state concentration of virus was only reduced to 85 ± 20 percent of the input. Aluminum metal appears to be orders of magnitude more effective.

After ~300 bed volumes, the organics in the secondary effluent plus those from the 1% fetal bovine serum used to stabilize the input virus inoculum failed to block steady-state virus removal by Al metal. Operation of an adsorption-filtration unit process may eventually be hindered, however, by long-term buildup of organic films. Before making a realistic estimate of the cost-effectiveness of Al metal for virus removal, answers to the potential surface coating problem must be obtained. Al metal effervesces on reaction with both acid and base in aqueous systems. This might well be incorporated into backwashing operations, to strip minor amounts of the metal plus organic films from the surface, greatly extending the useful operation of the process metal.

This investigation has demonstrated that Al metal is effective in removing poliovirus type 1, strain LSc2ab from wastewater. Further investigation is clearly needed to demonstrate effectiveness with other viruses, especially hepatitis type A. Finally, engineering optimization studies are needed to determine whether or not unit processes are cost-effective compared to other potentially safe virus removal operations.

REFERENCES

1. Goldfield, M. Epidemiological Indicators for Transmission of Viruses by Water. In: Viruses in Water, G. Berg, H. L. Bodily, E. H. Lennette, J. L. Melnick, and T. G. Metcalf, eds. Amer. Pub. Health Assoc., Washington, D.C., 1976, pp. 70-85.

2. Melnick, J. L. Detection of Virus Spread by the Water Route. In: Viruses and Water Quality: Occurrence and Control, V. Snoeyink and V. Griffin, eds. Univ. Ill. Bull. Vol. 69, No. 1, Urbana, Ill., 1971. pp. 114-125.

3. Stone, E. M., et al. A Waterborne Epidemic of Salmonellosis in Riverside, California, 1965. Amer. Jour. Epidem. 93 (1): 33-54, 1971.

4. Berg, G. Integrated Approach to Problem of Viruses in Water. J. Sanit. Engr. Div., Amer. Soc. Civil Engr. 79 (SA6): 867-882, 1971.

5. Denis, F. Incidences Epidémiologiques de la Contamination Virale des Aux. Rev. Epidém., Méd. Soc. et Santé Publ. 21 (4): 273-302, 1973.

6. Plotkin, S. A., and M. Katz. Minimal Infective Doses of Viruses for Man by the Oral Route. In: Transmission of Viruses by the Water Route, G. Berg, ed. Interscience, New York, 1967. pp. 151-166.

7. Drewry, W. A. An Experimental and Theoretical Study of the Movement of Viruses through Groundwater. Ph.D. Thesis, Stanford University, Stanford, Calif., 1968. 150 pp.

8. Ryan, W. Studies of the Movement of Viruses through Groundwater. Engr. Thesis, Stanford University, Stanford, Calif., 1967. 137 pp.

9. Cookson, J. T., and W. J. North. Adsorption of Viruses on Activated Carbon. Environ. Sci. Tech. 1 (1): 46-52, 1967.

10. Cookson, J. T. Adsorption of Viruses on Activated Carbon. Environ. Sci. Tech. 1 (2): 157-160, 1967.

11. Gerba, C. P., C. Wallis, and J. L. Melnick. Fate of Wastewater Bacteria and Viruses in Soil. J. Irrig. Div. Amer. Soc. Civil Engr., 101 (IR3): 157-174, 1975.

12. Warren, J., M. Kende, and K. Takano. The Adjuvant Effect of Powdered Ferric Oxide: Enhancement of Response of Mycoplasma Pneumoniae and Respiratory Syncytial Virus Vaccines. J. Immun. 102 (5): 1300-1308, 1969.

13. Mitchell, R., and H. W. Jannasch. Processes Controlling Virus Inactivation in Seawater. Environ. Sci. Tech. 3 (10): 941-943, 1969.

14. Smith, E. M., C. P. Gerba, and J. L. Melnick. Role of Sediment in the Persistence of Enteroviruses in the Estuarine Environment. Appl. Environ. Microbiol. 35 (4): 685-693, 1978.

15. Schaub, S. A., and B. P. Sagik. Association of Enteroviruses with Natural and Artificially Introduced Colloidal Solids in Water, and Infectivity of Solids Associated Virions. Appl. Microbiol. 30 (2): 212-222, 1975.

16. Environmental Protection Agency. Preliminary Assessment of Suspected Carcinogens in Drinking Water - Report to Congress, December, 1975.

17. Page, T., R. Harris, and J. Bruser. Removal of Carcinogens from Drinking Water: A Cost-Benefit Analysis. California Inst. Technology Social Science Working Paper 230, 1979, 82 pp.

18. Simmon, V. F., K. Kauhanen, and R. Tardiff. Mutagenic Activity of Chemicals Identified in Drinking Water. In: Progress in Genetic Toxicology, D. Scott, B. A. Bridges, and F. Sobels, eds. Elsevier - North Holland, Biomedical Press, New York. pp. 249-258, 1977.

19. Gruener, N. Mutagenicity of Ozonated, Recycled Water. Bull. Environm. Contam. Toxicol. 20: 522-526, 1978.

20. Derjaguin, B., and L. D. Landau. Theory of the Stability of Strongly Charged Lyophobic Sols and of the Adhesion of Strongly Charged Particles in Solutions of Electrolytes. Acta Physicochim. U.R.S.S. 14: 633, 1941.

21. Verwey, E. J. W., and Overbeek, J. Th. G. Theory of the Stability of Lyophobic Colloids. Elsevier, New York, 1948. 205 pp.

22. Dzyaloshinski, I. E., E. M. Lifshitz, and L. P. Pitaevski. The General Theory of Van der Waals Forces. Adv. Phys. 10 (37): 165-209, 1961.

23. Fenner, F., B. R. McAuslan, C. A. Mims, J. Sambrook, and D. O. White. The Biology of Animal Viruses, 2nd ed. Academic Press, New York, 1974. 834 pp.

24. England, B., R. E. Leach, B. Adame, and R. Shinosaki. Virologic Assessment of Sewage Treatment at Santee, Calif. In: Transmission of Viruses by the Water Route, G. Berg, ed. Interscience, New York, 1967. pp. 401-417.

25. Chang, S. L. Statistics of the Infectious Units of Animal Viruses. In: Transmission of Viruses by the Water Route, G. Berg, ed. Interscience, New York, 1967. pp. 219-234.

26. Schwerdt, C. E., and F. L. Schaffer. Purification of Poliomyelitis Viruses Propagated in Tissue Culture. Virol. 2 (5): 665-678, 1956.

27. McClain, M. E., and C. E. Schwerdt. Use of HeLa Cells for Plaque Assay of Poliomyelitis Virus. Fed. Proc. Amer. Soc. Exptl. Biol. 13 (1): 505, 1954.

28. White, A., P. H. Handler, and E. L. Smith. Principles of Biochemistry, 5th ed. McGraw-Hill, New York, 1973. pp. 806.

29. Charney, J., R. A. Machlowitz, and D. S. Spicer. The Adsorption of Poliovirus Antigen to Glass Surfaces. Virol. 18 (3): 495-497, 1962.

30. Charney, J., R. Machlowitz, A. A. Tytell, J. F. Sagin, and D. S. Spicer. The Concentration and Purification of Poliomyelitis Virus by Use of Nucleic Acid Precipitation. Virol. 15 (3): 269-280, 1961.

31. Maizel, J. V., and D. Summers. Evidence for Differences in Size and Composition of the Poliovirus Specific Polypeptides in Infected HeLa Cells. Virol. 36 (1): 48-54, 1968.

32. Joklik, W. K., and J. E. Darnell. The Adsorption and Early Fate of Purified Poliovirus in HeLa Cells. Virol. 13 (4): 439-447, 1961.

33. Wang, C. H., D. L. Willis, and W. D. Loveland. Radiotracer Methodology in the Biological, Environmental, and Physical Sciences. Prentiss-Hall, Englewood Cliffs, N.J., 1975. 480 pp,

34. Murray, J. P. Thermodynamics of Poliovirus Adsorption. Ph.D. Thesis, Stanford University, Stanford, Calif., 1978. 196 pp.

35. Stumm, W. and J. J. Morgan. Aquatic Chemistry. Interscience, New York, 1970. 583 pp.

36. Wiese, G. R., and T. W. Healy. Solubility Effects in Al_2O_3 and TiO_2 Colloidal Dispersions. J. Colloid Interface Sci. 52 (3): 452-457, 1975.

37. Wagman, D. D., W. H. Evans, V. B. Parker, I. Halow, S. M. Bailey, and R. H. Schumm. Selected Values of Chemical Thermodynamic Properties. N.B.S. Tech. Note 270-3. U.S. Govt. Print. Office, Washington, D.C., 1968. 264 pp.

38. DiStephano, T. H., and D. E. Eastman. Photoemission Measurements of the Valence Levels of Amorphous SiO_2 . Phys. Rev. Letters 27 (23): 1560-1562. 1971.

39. Taras, M. J., A. E. Greenberg, R. D. Hoak, and M. C. Rand. Standard Methods for the Examination of Water and Wastewater, 13th ed. Amer. Public Health Assoc., Washington, D.C., 1971. 874 pp.

40. Dhar, H. P., B. E. Conway, and K. M. Joshi. On the Form of Adsorption Isotherms for Substitutional Adsorption of Molecules of Different Sizes. Electrochim. Acta. 18 (11): 789-798, 1973.

41. Brunauer, S., P. Emmett, and E. Teller. Adsorption of Gases in Multimolecular Layers. J. Amer. Chem. Soc. 60 (2): 309-319, 1938.

42. Jura, G. The Determination of the Area of the Surfaces of Solids. In: Physical Methods in Chemical Analysis, Vol. 2., W. G. Berl, ed. Academic Press, New York. 1951. pp. 255-303.

43. Vuceta, J. Adsorption of Pb(II) and Cu(II) on α-Quartz from Aqueous Solutions: Influence of pH, Ionic Strength, and Complexing Ligands. Ph.D. Thesis, Calif. Inst. of Tech., Pasadena, Calif. 1976. 206 pp.

44. O'Melia, C. R., and W. Stumm. Aggregation of Silica Dispersions by Iron(III). J. Colloid Interface Sci. 23 (3): 437-447, 1967.

45. American Association for Testing Materials. Standard Methods for Test of Fineness for Portland Cement by Air Permeability Apparatus, C-204-73. Vol. 13, 1973, pp. 182-188.

46. Schultz, N. F. Measurement of Surface Areas by Permeametry. Internat. J. Min. Proc. 1: 65-79, 1974.

47. Parks, G. A. Adsorption in the Marine Environment. In: Chemical Oceanography, Vol. 1, G. Riley and G. Skirrow, eds. Academic Press, New York, 1976. pp. 241-308.

48. Gregory, J. Interaction of Unequal Double Layers at Constant Charge. J. Colloid Interface Sci. 51 (1): 44-51, 1975.

49. Smith, A. L. Electrokinetics of the Oxide Solution Interface. J. Colloid Interface Sci. 55 (3): 525-530, 1976.

50. Visser, J. The Adhesion of Colloidal Polystyrene Particles to Cellophane as a Function of pH and Ionic Strength. J. Colloid Interface Sci. 55 (3): 664-677, 1976.

51. Wiersema, P. H., A. L. Loeb, and J. Th. G. Overbeek. Calculation of the Electrophoretic Mobility of a Spherical Colloid Particle. J. Colloid Interface Sci. 22 (1): 78-99, 1966.

52. Hunter, R. J., and H. J. L. Wright. The Dependence of Electrokinetic Potential on Concentration of Electrolyte. J. Colloid Interface Sci. 37 (3): 564-580, 1971.

53. Murray, J. P. and C. E. Schwerdt. Calculation of Zeta Potentials of Suboptical Particles by Electrophoresis in Sucrose Gradients. Unpub. Res. 1978.

54. Yates, D. E., S. Levine, and T. Healy. Site-Binding Model of the Electrical Double Layer at the Oxide/Water Interface. J. Chem. Soc. Faraday Trans. I. 70: 1807-1818, 1974.

55. LaColla, P., M. Marcialis, G. P. Mereu, and B. Loddo. Behavior of a Guanidine-Dependent Strain of Poliovirus 1 in Sucrose Density and pH Gradients. Experientia 28 (9): 1115-1117, 1972.

56. Mandel, B. Characterization of Type 1 Poliovirus by Electrophoretic Analysis. Virol. 44 (3): 554-568, 1971.

57. Ward, R. L. Mechanism of Poliovirus Inactivation by Ammonia. J. Virol. 26 (2): 299-305, 1978.

58. Floyd, R., and D. G. Sharp. Viral Aggregation: Effects of Salts on the Aggregation of Poliovirus and Reovirus at Low pH. Appl. Environ. Microbiol. 35 (6): 1084-1094, 1978.

59. Young, D. C., and D. G. Sharp. Presented at ASM National Meeting, Honolulu, 1979.

60. Lipatov, Yu. S., and L. M. Sergeeva. Adsorption of Polymers. Halsted Press, New York, 1974. 177 pp.

61. Parsegian, V. A. Long Range Van der Waals Forces. In: Physical Chemistry: Enriching Topics from Colloid and Surface Science, H. van Olphen and K. Mysels, eds., I.U.P.A.C. 1.6, Theorex, La Jolla, Calif., pp. 27-72, 1975.

62. Richmond, P. The Theory and Calculation of Van der Waals Forces. In: Colloid Science, Vol. 2, D. Everett, ed. The Chem. Soc., London, 1974. pp. 130-172.

63. Hamaker, H. C. The London-Van der Waals Attraction between Spherical Particles. Physica IV (10): 1058-1072, 1937.

64. Bargeman, D. and F. Van Voorst Vader. Van der Waals Forces between Immersed Particles. J. Electroanal. Chem. Interfacial Electrochem. 37 (1): 42-52, 1972.

65. Visser, J. Adhesion of Colloidal Particles. In: Surface and Colloid Sci., Vol. 8, Chap. 1, E. Matijevic, ed. Interscience, New York, 1976. pp. 3-84.

66. Ninham, B., and V. A. Parsegian. Van der Waals Forces, Special Characteristics in Lipid-Water Systems and a General Method of Calculation Based on Lifshitz Theory. Biophys. J. 10: 646-674, 1970.

67. van Oss, C. J., et al. Comparison between Attachment and Detachment Approaches to the Quantitative Study of Cell Adhesion to Low-Energy Solids. J. Colloid Interface Sci., 59 (3): 505-515, 1977.

68. Lukěs, F. Oxidation of Si and GaAs in Air at Room Temperature. Surface Sci. 30 (1): 91-100, 1972.

69. Smith, T. Auger Electron Spectroscopy and Ion Sputter Profiles of Oxides on Aluminum. Surface Sci. 55 (2): 601-624, 1976.

70. Murray, J. P., and G. A. Parks. Poliovirus Adsorption of Oxide Surfaces - Correspondence with the DLVO-Lifshitz Theory of Colloid Stability. A.C.S. Adv. in Chem. Series, Particulates in Water. M. Kavanaugh and J. Leckie, eds. In Press, 1980.

71. LeNeveu, D. M., R. Rand, V. Parsegian, and D. Gingell. Measurement and Modification of Forces between Lethicin Bilayers. Biophys. J. 18: 209-230, 1977.

72. Wallis, C., and J. L. Melnick. Concentration of Viruses on Aluminum Phosphate and Aluminum Hydroxide Precipitates. In: Transmission of Viruses by the Water Route, G. Berg, ed. Interscience, New York, 1967. pp. 129-138.

73. Gerba, C. P., M. Sobsey, C. Wallis, and J. L. Melnick. Adsorption of Poliovirus onto Activated Carbon in Wastewater. Env. Sci. Tech. 9 (8): 727-731, 1975.

74. Hill, W. F., E. W. Akin, and W. H. Benton. Detection of Viruses in Water: A Review of Methods and Application. In: Virus and Water Quality: Occurrence and Control, V. Snoeyink and V. Griffin, eds., Univ. Ill. Bull. Vol. 69, No. 1, Urbana, Ill., 1971. pp. 17-46.

75. McEwen, C. R. Tables for Estimating Sedimentation through Linear Concentration Gradients of Sucrose Solution. Anal. Biochem. 20 (1): 114-149, 1967.

76. Jordan, L., and H. D. Mayor. Studies on the Degradation of Poliovirus by Heat. Microbios 9 (33-34): 51-60, 1971.

77. Stone, M. R. Studies on the Reconstitution and Structure of Three Strains of Poliovirus Type I. Ph.D. Thesis, Stanford University, Stanford, Calif., 1977. 175 pp.

78. Brown, T. S., J. F. Malina, B. D. Moore, and B. P. Sagik. Virus Removal by Diatomaceous Earth Filtration. In: Virus Survival in Water and Wastewater Systems, J. Malina and B. Sagik, eds. Univ. Texas Press, Austin, 1974. pp. 129-144.